Evolution of specialization in heterogeneous environments: equilibrium between selection, mutation and migration

Sepideh Mirrahimi, Sylvain Gandon

Evolution of specialization in heterogeneous environments: equilibrium between selection, mutation and migration

Sepideh Mirrahimi [*] Sylvain Gandon[†]

Abstract

Adaptation in spatially heterogeneous environments results from the balance between local selection, mutation and migration. We study the interplay among these different evolutionary forces and demography in a classical two-habitat scenario with asexual reproduction. We develop a new theoretical approach that goes beyond the Adaptive Dynamics framework and allows us to explore the effect of high mutation rates on the stationary phenotypic distribution. We show that this approach improves the classical Gaussian approximation and captures accurately the shape of this equilibrium phenotypic distribution in one and two-population scenarios. We examine the evolutionary equilibrium under general conditions where demography and selection may be non-symmetric between the two habitats. In particular, we show how migration may increase differentiation in a source-sink scenario. We discuss the implications of these analytic results for the adaptation of organisms with large mutation rates such as RNA viruses.

Key-Words: local adaptation, migration-selection balance, gene flow, Adaptive Dynamics, Quantitative Genetics, skew.

1 Introduction

Spatially heterogeneous selection is ubiquitous and constitutes a potent evolutionary force that promotes the emergence and the maintenance of biodiversity. Spatial variation in selection can yield adaptation to local environmental conditions, however, other evolutionary forces like migration and mutation tend to homogenize the spatial patterns of differentiation and thus to impede the build up of local adaptation. Understanding the balance between these contrasted evolutionary forces is a major objective of evolutionary biology theory Slatkin 1978; Whitlock 2015; Savolainen et al. 2013) and could lead to a better understanding of the speciation process and the evolutionary response to global change Doebeli and Dieckmann 2003; Leimar et al. 2008. In this article, we consider a two-habitat model with explicit demographic dynamics as in Meszéna et al. 1997; Day 2000; Ronce and Kirkpatrick 2001; Débarre et al. 2013. We assume that adaptation is governed by a single quantitative trait where individuals reproduce asexually. Maladapted populations have a reduced growth rate and, consequently, lower population size. In other words, selection is assumed to be 'hard' Christiansen 1975; Débarre and Gandon 2010 as the population size in each habitat is affected by selection, mutation and migration. These effects are complex because, for instance, non-symmetric population sizes affect gene flow and adaptation feeds back on demography and population sizes Nagylaki 1978; Lenormand 2002; Meszéna

[*]Institut de Mathématiques de Toulouse, UMR5219, Université de Toulouse, CNRS, UPS, IMT, F-31062 Toulouse Cedex 9, France

[†]CEFE UMR 5175, CNRS – Université de Montpellier, Université Paul-Valéry Montpellier, EPHE, 1919, route de Mende, 34293 Montpellier Cedex 5, France

et al. 1997; Day 2000; Ronce and Kirkpatrick 2001; Débarre et al. 2013. To capture the complexity of these feed backs it is essential to keep track of both the local densities and the distributions of phenotypes in each habitat. Note that this complexity often led to the analysis of the simplest ecological scenarios where the strength of selection, migration and demographic constraints are assumed to be the same in the two habitats (we will refer to such situations as symmetric scenarios). See however Holt and Gaines 1992; García-Ramos and Kirkpatrick 1997; Gomulkiewicz et al. 1999; Holt et al. 2003 for the analysis of the effect of asymmetric migration from a source habitat on the dynamics of adaptation in a peripheral (i.e. sink) habitat. Three different approaches have been used to analyze these two-population models. Each of these approaches rely on a set of restrictive assumptions regarding the relative influence of the different evolutionary forces acting on the evolution of the population.

First, under the assumption that the rate of mutation is weak relative to selection, it is possible to use the Adaptive Dynamics framework (see Meszéna et al. 1997; Day 2000; Szilágyi and Meszéna 2009; Débarre et al. 2013; Fabre et al. 2012 and also sections 3.1.1 and 3.2.1 for a presentation of this framework). This analysis captures the effect of migration and selection on the long-term evolutionary equilibrium. In particular, this approach shows that weak migration relative to selection promotes the coexistence of two specialist strategies (locally adapted on each habitat). In contrast, when migration is strong relative to selection, a single generalist strategy is favored. The main limit of this approach is that it relies on the assumption that mutation rate is vanishingly small which results in a very limited amount of genetic variability. At most, 2 genotypes can coexist in this two-habitat model.

Second, Quantitative Genetics formalism, based on the computation of the moments of the phenotypic distribution, has been used to track evolutionary dynamics in heterogeneous habitats when there is substantial level of phenotypic diversity in each population Ronce and Kirkpatrick 2001. This model considers sexual reproduction with a quantitative trait (considering multiple loci with small effects Fisher 1919). However, similar types of equations, describing the dynamics of the moments of the phenotypic distribution, can also be derived in the case of asexual reproduction considering large mutation rates (see Débarre et al. 2013 and Section 3.2). This formalism allows to recover classical migration thresholds below which specialization is feasible. But the analysis of Ronce and Kirkpatrick 2001 also reveals the existence of evolutionary bistability where transient perturbations of the demography can have long term evolutionary consequences on specialization. Yet, the assumption on the shape of the phenotypic distribution (assumed to be Gaussian in each habitat) is a major limit of this formalism.

Third, attempts to account for other shapes of the phenotypic distributions in heterogeneous environments have been developed recently Yeaman and Guillaume 2009; Débarre et al. 2013, 2015. These models highlight that calculations based on the Gaussian approximation which neglects the skewness of the equilibrium phenotypic distribution under-estimates the level of phenotypic divergence and local adaptation. Yet, there is currently no model able to accurately describe the build up of non-Gaussian distributions. The only attempt to model this distribution is to describe the phenotypic distributions in each habitat as the sum of two Gaussian distributions Yeaman and Guillaume 2009; Débarre et al. 2013. These models, however, only yield approximate predictions on long-term evolutionary equilibria.

Here we develop an alternative formalism that yields the population size and the phenotypic distribution in each habitat at the equilibrium between selection, mutation and migration. In Section 2 we present our two-population model.For heuristic reasons, we next provide the analysis of the equilibrium between selection and mutation in a single population. This provides an illustration of our approach in a simple scenario and shows how this analysis can go beyond the classical Gaussian approximation. Next, we extend this approach to a two-population scenario where migration can also influence the phenotypic distribution, and we derive approximations for the level of adaptation under

a migration-selection-mutation balance. We also explore the effects of non-symmetric constraints on selection, migration or demography between the two habitats. We evaluate the accuracy of these approximations by comparing them to numerical solutions of our deterministic model and we show that our approach improves previous attempts to study the interplay between adaptation and demography in heterogeneous environments. We contend that our results are particularly relevant for organisms with high mutation rates and may help to understand the within-host dynamics of chronic infections by RNA viruses Drake and Holland 1999; Sanjuán et al. 2010.
The present work has been prepared in parallel to the mathematical article Mirrahimi 2017 where we provide the mathematical basis and proofs for the method used here. See also Gandon and Mirrahimi 2016 where those mathematical results were announced. The aim of the present paper is to show how this approach can help to understand the balance between different evolutionary forces. We present several new biological scenarios and we derive new results that help grasp the interplay between different evolutionary forces and demography.

2 Materials and Methods

We model an environment containing two habitats that we label 1 and 2 (Figure 1). The population is structured by a quantitative trait z. In each habitat i there is stabilizing selection on the trait z for an optimal value θ_i (for habitat $i = 1, 2$). The growth rate in habitat i is denoted by $r_i(z)$ which has its maximum $r_{\max,i}$ when $z = \theta_i$. In the following we will mainly focus on the following quadratic stabilizing selection function (Bürger 2000– pages 117-121 and chapter VI):

$$r_i(z) = r_{\max,i} - s_i \left(z - \theta_i\right)^2 . \tag{1}$$

We denote by s_i the selection pressure in habitat i. Without loss of generality we assume that $\theta_1 = -\theta_2 = -\theta$. But our approach could be used with other stabilizing selection functions (see (12) below where another selection function is studied in the case of one population).

Reproduction is assumed to be asexual. Offspring inherit the phenotype of their parent (i.e. no environmental variance) and we consider a continuum of alleles model Kimura 1965. Mutations occur with a constant rate U (i.e. mutations are not associated with reproduction) and add an increment y to the parents' phenotype; we assume that the distribution of these mutational effects is given by $K(y)$, with mean 0 and variance equal to $2V_m$. We also assume that individuals disperse out of habitat i with rate m_i. Rates of migration are assumed to be independent of individuals' phenotypes.

Let $n_i(t, z)$ be the phenotypic density in habitat i at time t. The dynamics of this density in each habitat is given by (for $i = 1, 2$ and $j = 2, 1$):

$$\begin{aligned} \frac{\partial n_i(t,z)}{\partial t} &= \underbrace{U\Big(\int_{-\infty}^{+\infty} n_i(t, z-y)K(y)dy - n_i(t,z)\Big)}_{\text{mutation}} \\ &+ \underbrace{n_i(t,z)\left(r_i(z) - \kappa_i \int_{-\infty}^{+\infty} n_i(t,y)dy\right)}_{\text{growth}} + \underbrace{m_j n_j(t,z) - m_i n_i(t,z)}_{\text{migration}} . \end{aligned} \tag{2}$$

The first term in the right hand side of the above equation corresponds to the effect of mutations. The

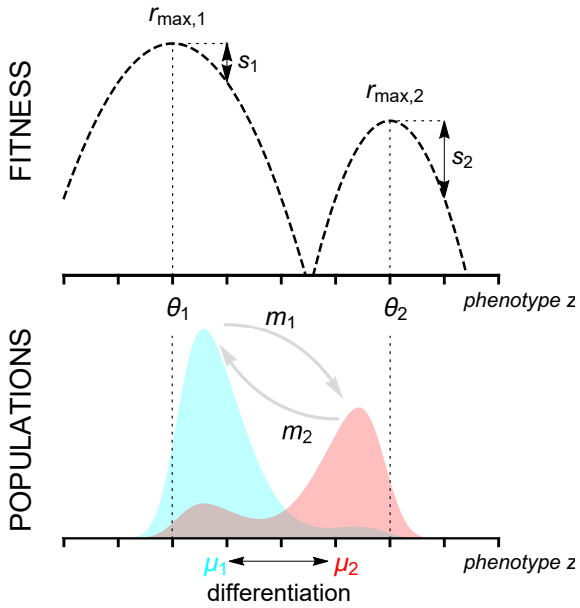

Figure 1 – Schematic representation of the 2 habitat model. The top figure shows the growth rate (fitness) in each habitat as a function of the phenotypic trait z. In habitat i the growth rate is assumed to be maximized at $z = \theta_i$ and the strength of selection is governed by s_i (see equation (1)). Here we illustrate a scenario with non-symmetric fitness functions. The bottom figure shows the phenotypic density in each habitat (light blue and light red in habitats 1 and 2, respectively). Migration from population i is governed by the parameter m_i and tends to reduce the differentiation (i.e. the difference between the mean phenotypes) between populations.

second term corresponds to logistic growth that results from the balance between reproduction given by (1) and density dependance where κ_i measures the intensity of competition within each habitat. The last term corresponds to the dispersal of individuals between habitats.
If we assume that the variance of the mutation distribution is small relative to the mutation rate U, we can consider an approximate model where we replace the mutation term in (2) by a diffusion (see Kimura 1965; Lande 1975 and the more recent article Champagnat et al. 2008 where the diffusion term has been derived directly from a stochastic individual based model). See also Bürger 2000–pages 239-241 for a discussion on the domain of the validity of such model. Our model then becomes:

$$\frac{\partial n_i(t,z)}{\partial t} = UV_m \frac{\partial^2 n_i(t,z)}{\partial z^2} + n_i(t,z)\left(r_i(z) - \kappa_i \int_{-\infty}^{+\infty} n_i(t,y)dy\right) + m_j n_j(t,z) - m_i n_i(t,z). \qquad (3)$$

The total population sizes in each habitat is given by:

$$N_i(t) = \int_{-\infty}^{+\infty} n_i(t,z)dz, \qquad \text{for } i = 1,2. \qquad (4)$$

In other words, $n_i(t,z)$ refers to the density of individuals with phenotype z in habitat i, while N_i refers to the total density of the polymorphic population in habitat i.

Data availability No biological data is provided in this article.

3 Results

3.1 One population: the selection-mutation equilibrium

In this section we start by a simple scenario with no migration. This one-population example provides a good introduction to our method. The dynamics of the phenotypic density in a single habitat is given by:

$$\frac{\partial n_0(t,z)}{\partial t} = UV_m \frac{\partial^2 n_0(t,z)}{\partial z^2} + n_0(t,z)\left(r_0(z) - \kappa N_0(t)\right), \tag{5}$$

where N_0 is the total population size:

$$N_0(t) = \int_{-\infty}^{+\infty} n_0(t,y)dy.$$

For this scenario we consider a more general form of growth rate $r_0(z)$ than (1). We only suppose that $r_0(z)$ is maximized for an optimal trait z_0. In the following we present our two-step approach. First, we analyse the evolutionary equilibria of the problem when the rate of mutation is small and we identify the evolutionary stable strategy (ESS). Second, we use this ESS to derive an approximation for the stationary solution of (5) when mutation is more frequent and maintains a standing variance at equilibrium.

3.1.1 Adaptive dynamics and evolutionary stable strategies

In this section, we assume that the mutations are very rare such that a mutation is fixed or goes extinct before a new mutation arises in the population. The phenotypic distribution results from a collection of spikes. Such spikes are gradually replaced by others with the arrival of new mutations and through a competitive procedure. The theory of Adaptive Dynamics Geritz et al. 1998 is based on the study of the stable equilibrium distribution and the localization of the spikes of such equilibrium, known as evolutionary stable strategies (ESS). Note that in this first step we do not make any assumption regarding the effects of these mutations on the phenotype. We are interested in the identification of the global ESSs, i.e. when the resident population cannot be invaded by any mutation no matter its effect.

In absence of migration, the phenotype z_0 constitutes a globally stable evolutionary strategy. Indeed, when such monomorphic population reaches its demographic equilibrium, the total population size is given by $N_0^* = \frac{r(z_0)}{\kappa}$. The fate of a mutant with phenotype z_m introduced in such a resident population is determined by its fitness given by (i.e. per capita growth rate minus density dependence):

$$w(z_m; N_0^*) = r_0(z_m) - \kappa_0 N_0^* < w(z_0; N_0^*) = 0. \tag{6}$$

No mutant trait z_m can indeed invade the population since $r_0(z)$ takes its maximum at z_0.

3.1.2 Equilibrium distribution with mutation

The ESS z_0 corresponds to the long-term evolutionary outcome in a scenario where all phenotypic strategies are present initially but where mutation is absent. In the following we study the impact of

mutation on the ultimate evolutionary equilibrium of the population.
We introduce a new parameter $\varepsilon = \sqrt{V_m}$. Hence we replace V_m by ε^2 and we approximate the phenotypic density $n^*_{\varepsilon,0}(z)$, the equilibrium of (5), in terms of ε (where the subscript ε in $n^*_{\varepsilon,0}$ indicates the dependence of the phenotypic density on the parameter ε). Our objective is to provide an approximation of the phenotypic density when the effect of mutation (measured by ε) is small while the mutation rate can be large.
To study $n^*_{\varepsilon,0}(z)$ we will use a method based on Hamilton-Jacobi equations (see equation (A.5)) which has been developed by the mathematical community during the last decade to study selection-mutation models, when the effect of mutations is vanishingly small. This method was first suggested by Diekmann et al. 2005 and was developed for the case of homogeneous environments in Perthame and Barles 2008; Barles et al. 2009. However those works, which are addressed to the mathematical community, were mainly focused on the limit case where the effect of mutations ε is vanishingly small. Here, we go further than previous studies and characterize the phenotypic distribution when the mutations have non-negligible effects.
The method is based on the following transformation:

$$n^*_{\varepsilon,0}(z) = \frac{1}{\sqrt{2\pi\varepsilon}} \exp\Big(\frac{u_{\varepsilon,0}(z)}{\varepsilon}\Big). \tag{7}$$

The introduction of the function $u_{\varepsilon,0}(z)$ is a mathematical trick. It is indeed easier to provide first an approximation of $u_{\varepsilon,0}(z)$ rather than directly studying $n^*_{\varepsilon,0}(z)$.
Note that a first approximation of the population's phenotypic density which is commonly used in the theory of Quantitative Genetics is a Gaussian approximation of the following form around z^*:

$$n^*_{\varepsilon,0}(z) \approx N^*_{\varepsilon,0}\,\mathcal{N}(z^*, \varepsilon\,\sigma^2). \tag{8}$$

The Gaussian approximation, is as if we had imposed $u_{\varepsilon,0}(z)$ to be a quadratic function of z, that is $u_{\varepsilon,0}(z) = \varepsilon \log(\frac{N^*_{\varepsilon,0}}{\sigma}) - \frac{(z-z^*)^2}{2\sigma^2}$. Our objective, however, is to obtain more accurate results than (8) and to approximate $u_{\varepsilon,0}$ without making an a priori Gaussian assumption. To this end we postulate an expansion for $u_{\varepsilon,0}(z)$ in terms of ε:

$$u_{\varepsilon,0}(z) = u_0(z) + \varepsilon v_0(z) + O(\varepsilon^2), \tag{9}$$

and we try to compute the coefficients $u_0(z)$ and $v_0(z)$. These terms can indeed be explicitly computed and they lead to an approximation of the total population size N^*_ε and the phenotypic density $n^*_\varepsilon(z)$ that we will call henceforth our *first approximation* (see the supplementary information A.1.1 for these derivations).
In order to provide more explicit formula for the moments of order $k \geq 1$ of the population's distribution in terms of the parameters of the model, we also provide a *second approximation*. This *second approximation*, instead of using the values of u_0 and v_0 in the whole domain, is based on the Taylor expansions of u_0 and v_0 around the ESS points (see the supplementary information, Section A.1.2). Our *second approximation* is by definition less accurate than the first one. We illustrate below the quality of these different approximations under two different scenarios.

Quadratic growth rate: We first consider a quadratic growth rate as in (1):

$$r_0(z) = r_{\max,0} - s_0(z-\theta_0)^2. \tag{10}$$

In this case our *first approximation* yields the Gaussian distribution (8) with:

$$N^*_{\varepsilon,0} \approx \frac{1}{\kappa_0}(r_{\max,0} - \varepsilon\sqrt{s_0 U}), \qquad \sigma^2 \approx \frac{\sqrt{U}}{\sqrt{s_0}}. \tag{11}$$

Note that this Gaussian distribution is actually an exact equilibrium of (3) and the above $\approx$ signs can indeed be replaced by equalities (see Kimura 1965 and Bürger 2000–Chapter IV). For the derivation of this result see the supplementary information–Section A.1.1.

An asymmetric growth rate: We next consider a growth rate which is not symmetric:

$$r_0(z) = r_{\max,0} - s_0(z-\theta_0)^2\big(a + (z-\theta_0-b)^2\big). \tag{12}$$

In this case the phenotypic distribution does not have a Gaussian profile and our approximation yields:

$$N^*_{\varepsilon,0} \approx \frac{1}{\kappa_0}(r_{\max,0} - \sqrt{s_0 U(a+b^2)}\,\varepsilon), \qquad n^*_{\varepsilon,0}(z) \approx \frac{1}{\sqrt{2\pi\varepsilon}} \exp\Big(\frac{u_0(z) + \varepsilon v_0(z)}{\varepsilon}\Big),$$

where the values of u_0 and v_0 can be computed explicitly (see the supplementary information–Section A.1.1). In Figure 2 we plot this *first approximation* and compare it with the exact distribution that we derived numerically.
We can also use our *second approximation* to obtain analytic expressions for the mean phenotypic trait (see the supplementary information-Section A.1.2 for the derivation):

$$\mu^*_{\varepsilon,0} = \frac{1}{N^*_{\varepsilon,0}} \int z n^*_{\varepsilon,0}(z)dz = \theta_0 + \frac{2b\sqrt{U}\varepsilon}{\sqrt{s_0}(a+b^2)^{3/2}} + O(\varepsilon^2),$$

the mean variance:

$$\sigma^{*2}_{\varepsilon,0} = \frac{1}{N^*_{\varepsilon,0}} \int (z-\mu^*_{\varepsilon,0})^2 n^*_{\varepsilon,0}(z)dz = \frac{\sqrt{U}\varepsilon}{\sqrt{s_0(a+b^2)}} + O(\varepsilon^2),$$

and the third central moment:

$$\psi^*_{\varepsilon,0} = \frac{1}{N^*_{\varepsilon,0}} \int (z-\mu^*_{\varepsilon,0})^3 n^*_{\varepsilon,0}(z)dz = \frac{2bU\varepsilon^2}{s_0(a+b^2)^2} + O(\varepsilon^3).$$

In Table 1 we show that our two approximations capture accurately the first three moments of the equilibrium distribution using the parameters that we used in Figure 2. As expected, the *first approximation* is more accurate, but the analytic expressions of the *second approximation* given above allow us to capture the influence of the parameters of the model.

3.2 Two populations: the selection-mutation-migration equilibrium

Next we return to the analysis of the stationary solution of (3), which results from the equilibrium between selection, mutation and migration in each habitat. Using (1) and (3) one can derive dynamical

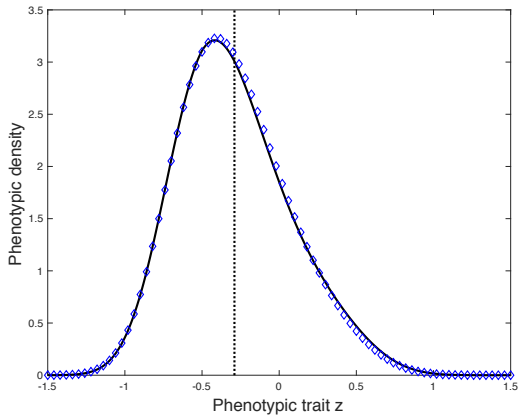

Figure 2 – The selection-mutation equilibrium of the phenotypic density $n_{\varepsilon,0}(z)$ in a single population. We plot the exact phenotypic density at equilibrium obtained from numerical computations of the equilibrium of (5) (blue dots) together with our *first approximation* (full black line) with the growth rate given in (12). The vertical dotted line indicates the mean of the phenotypic distribution. Note the skewness of the equilibrium distribution that is accurately captured with our approximation (see also Table 1). In this figure, to compute numerically the equilibrium, we have solved numerically the dynamic problem (5) and kept the solution obtained after long time when the equilibrium has been reached. Parameter values: $r_{\max} = 3$, $s_0 = 1$; $\theta = -0.5$, $\kappa = 1$, $a = 0.2$, $b = 1$, $U = 1$, $\varepsilon = 0.1$.

equations for the size of the population and the mean phenotype ($\mu_i = \frac{1}{N_i}\int z n_i(t,z)dz$):

$$\frac{d}{dt}N_i = N_i(r_{\max,i} - \kappa_i N_i) - s_i N_i\big((\mu_i - \theta_i)^2 + \sigma_i^2\big) + m_j N_j - m_i N_i,$$

$$\frac{d}{dt}\mu_i = -s_i\big(2(\mu_i - \theta_i)\sigma_i^2 + \psi_i\big) + m_j\frac{N_j}{N_i}(\mu_j - \mu_i),$$

where σ_i^2 and ψ_i are the variance and the third central moment of the phenotypic distribution, respectively. These two quantities are also dynamical variables and their dynamics are governed by higher moments of the phenotypic distribution. But this dynamical system is not closed and these higher moments are also dynamical variables that depend on additional moments. Various approximations, however, have been used to capture its behavior. Typically, many results are based on the Gaussian approximation that focuses on the dynamics of the mean and the variance and discards all higher cumulants of the distribution Bürger 2000; Rice 2004. Yet several authors pointed out that neglecting the skewness of the distribution can underestimate the amount of differentiation and local adaptation Yeaman and Guillaume 2009; Débarre et al. 2013, 2015. Indeed, in the case of symmetric habitats, that is when $m_1 = m_2 = m, \kappa_1 = \kappa_2 = \kappa, s_1 = s_2 = s, r_{\max,1} = r_{\max,2} = r_{\max}$, one can readily obtain the size and the mean trait of the population at equilibrium (the equilibrium is indicated by a superscript $*$). Using the fact that $N_1^* = N_2^* = N^*$, $\mu_1^* = -\mu_2^*$, $\sigma_1^* = \sigma_2^* = \sigma^*$ and $\psi_1^* = -\psi_2^* = \psi^*$, we obtain:

$$N^* = \frac{1}{\kappa}\Big(r_{\max} - s\Big(\frac{(2m\theta - s\psi^*)^2}{4(m + g\sigma^{*\,2})^2} + \sigma^{*\,2}\Big)\Big),$$

	Exact value	First approximation	Second approximation
Mean: $\mu^*_{\varepsilon,0}$	-0.29	-0.29	-0.35
Variance: $\sigma^{*2}_{\varepsilon,0}$	0.13	0.14	0.09
Third central moment: $\psi^*_{\varepsilon,0}$	0.02	0.02	0.01

Table 1 – First three moments of the phenotypic distribution at mutation-selection equilibrium in a single population. We compare the values from the exact numerical resolution of (5) and our two approximations using the growth rate given in (12) (see also Figure 2). Parameter values: $r_{\max} = 3$, $s_0 = 1$; $\theta = -0.5$, $\kappa = 1$, $a = 0.2$, $b = 1$, $U = 1$, $\varepsilon = 0.1$.

$$\mu_1^* = \frac{-s(\psi^* + 2\theta\sigma^{*\,2})}{2(m + s\sigma^{*\,2})}.$$

The differentiation between the two habitats is thus (Figure 1):

$$\mu_2^* - \mu_1^* = \frac{s(\psi^* + 2\theta\sigma^{*\,2})}{m + s\sigma^{*\,2}}. \tag{13}$$

There is, however, no analytic predictions on the magnitude of the different moments of the phenotypic distribution except in the limit when the mutation rate is extremely low Débarre et al. 2013.
Next, we follow the two-step approach we used to obtain the stationary phenotypic distribution in a single population. First, we analyse the evolutionary equilibria of the system when mutations are rare using the Adaptive Dynamics framework. We identify monomorphic or dimorphic globally evolutionary stable strategies (ESS). Second, we use these ESSs to derive approximations of the stationary solution of (3) when mutation is more frequent and maintains a standing variance at equilibrium.

3.2.1 Adaptive dynamics and evolutionary stable strategies

We consider a resident population at a demographic equilibrium set by the phenotypic densities of the resident in both habitats (see the supplementary information, Section A.2.1.1). We want to determine the fate of a mutant with phenotype z_m introduced in this resident population. The ability of the mutant to invade is determined by its fitness given by:

$$w_i(z_m; N_i) = r_i(z_m) - \kappa_i N_i, \qquad \text{for } i = 1, 2. \tag{14}$$

To take into account migration between habitats we introduce an effective fitness which corresponds to the growth rate of a trait in the whole environment (see Caswell 1989; Metz et al. 1992; Meszéna et al. 1997). The effective fitness $W(z_m; N_1, N_2)$, which corresponds to the *effective* growth rate associated with trait z_m in the resident population (n_1, n_2), is the largest eigenvalue of the following matrix:

$$\mathcal{A}(z_m; N_1, N_2) = \begin{pmatrix} w_1(z_m; N_1) - m_1 & m_2 \\ m_1 & w_2(z_m; N_2) - m_2 \end{pmatrix}. \tag{15}$$

After some time, the dynamical system will reach a globally stable demographic equilibrium. Because there are two habitats, we expect that at most two distinct traits can coexist. With an analysis of the effective fitness W, we characterize such equilibrium corresponding to the evolutionary stable strategy (see the supplementary information, Section A.2.1.1). This equilibrium is indeed either monomorphic (with phenotype z^{M*} and the total population size N_i^{M*}) or dimorphic (with phenotypes z_{I}^{D*} and z_{II}^{D*} and the total population sizes N_i^{D*}, where the subscripts I and II indicate that the phenotype is best adapted to habitat 1 and 2, respectively).

3.2.2 Equilibrium distribution with mutation

In the following we allow mutation rate to increase and we study the impact of mutations on the ultimate evolutionary equilibrium of the phenotypic densities, i.e. the stationary solution of (3). We present below the general principle of the approach before examining specific case studies.

As in Section 3.1.2 we introduce the parameter $\varepsilon = \sqrt{V_m}$ and we approximate the phenotypic density $n^*_{\varepsilon,i}(z)$, the equilibrium of (3) with $V_m = \varepsilon^2$, in terms of ε. Our objective is to provide an approximation of the phenotypic density in each habitat when the effect of mutation (measured by ε) is small while the mutation rate can be large.

We use analogous transformation to (7):

$$n^*_{\varepsilon,i}(z) = \frac{1}{\sqrt{2\pi\varepsilon}} \exp\big(\frac{u_{\varepsilon,i}(z)}{\varepsilon}\big). \tag{16}$$

Our objective is then to estimate $u_{\varepsilon,i}(z)$. We proceed as in Section 3.1.2 and we postulate an expansion for $u_{\varepsilon,i}$ in terms of ε:

$$u_{\varepsilon,i}(z) = u_i(z) + \varepsilon v_i(z) + O(\varepsilon^2), \tag{17}$$

and we try to compute the coefficients $u_i(z)$ and $v_i(z)$. First we can show that, when there is migration in both directions (i.e. $m_i > 0$ for $i = 1, 2$), the zero order terms are the same in both habitats: $u_1(z) = u_2(z) = u(z)$ (see the supplementary information, Section A.2.1.2). We can indeed compute explicitly $u(z)$ which is given by (A.23) in the monomorphic case and by (A.24) in the dimorphic case. As we observe in the formula (A.23) and (A.24), $u(z)$ attains its maximum (which is equal to 0) at the ESS points identified in the previous subsection. This means that the peaks of the population's distribution are around the ESS points (z^{M*} in the case of the monomorphic ESS and $(z_{\mathrm{I}}^{D*}, z_{\mathrm{II}}^{D*})$ for the dimorphic ESS). Note that the fact that $u_1(z) = u_2(z) = u(z)$ means that the peaks of the population distribution are placed approximately at the same points (ESS points) in both habitats. However, the size of the peaks may be different since $v_1(z)$ is not necessarily equal to $v_2(z)$.

We are also able to compute the first order term $v_i(z)$ (see the supplementary information, Section A.2.1.2). This allows us to obtain a *first approximation* of the phenotypic density $n^*_{\varepsilon,i}(z)$. This approximation of the stationary distribution is very accurate (see for instance Figure 4).

As in section 3.1.2 we derive more explicit formula for the moments of order $k \geq 1$ of the stationary phenotypic distribution. This *second approximation*, instead of using the values of $u(z)$ and $v_i(z)$ in the whole domain, is based on the computation of the Taylor expansions of $u(z)$ and $v_i(z)$ around the ESS points (see the supplementary information, Section A.2.1.3).

3.2.3 Case studies

Symmetric fitness landscapes

We focus first on a symmetric scenario where, apart from the position of the optimum, the two habitats are identical: $m_1 = m_2 = m, \kappa_1 = \kappa_2 = \kappa, s_1 = s_2 = s, r_{\max,1} = r_{\max,2} = r_{\max}$. In this special case it is possible to fully characterize the evolutionary equilibrium.

When migration rate is higher than critical migration threshold:

$$m > m_c = 2s\theta^2 \tag{18}$$

migration prevents the differentiation of the trait between the two habitats (see the supplementary information- Subsection A.2.1.1). The only evolutionary equilibrium, when the mutation rate is vanishingly small, is monomorphic and satisfies $z^{M*} = 0$ and $n_1^{M*}(z) = n_2^{M*}(z) = N^{M*}\delta(z)$, where $\delta(.)$ is the dirac delta function and $N^{M*} = \frac{1}{\kappa}\left(r_{\max} - s\theta^2\right)$.

Monomorphic case: Let's suppose that $m_c = 2s\theta^2 \leq m$. Then $z^{M*} = 0$ is the only ESS and $N^{M*} = \frac{1}{\kappa}\left(r_{\max} - s\theta^2\right)$. Then, we can provide our *first approximation* of the phenotypic density $n_{\varepsilon,i}(z)$ following the method introduced above (Figure 3). Moreover, defining $\phi = \sqrt{1 - 2s\theta^2/m}$, we can use the *second approximation* to obtain analytic formula for the moments of the stationary state:

$$\begin{cases} N_{\varepsilon,1}^{M*} = N_{\varepsilon,2}^{M*} = \int n_{\varepsilon,i}^{M*}(z)dz = \frac{1}{\kappa}\left(r_{\max} - s\theta^2\right) - \varepsilon\,\frac{\sqrt{Us}\,\phi}{\kappa} + O(\varepsilon^2), \\ \mu_{\varepsilon,1}^{M*} = \frac{1}{N_{\varepsilon,1}^{M*}}\int z n_{\varepsilon,1}^{M*}(z)dz = -\varepsilon\frac{\sqrt{Us}\,\theta}{m\phi} + O(\varepsilon^2), \\ \mu_{\varepsilon,2}^{M*} = \frac{1}{N_{\varepsilon,2}^{M*}}\int z n_{\varepsilon,2}^{M*}(z)dz = \varepsilon\frac{\sqrt{Us}\,\theta}{m\phi} + O(\varepsilon^2), \\ \sigma_{\varepsilon,1}^{M*\,2} = \sigma_{\varepsilon,2}^{M*\,2} = \frac{1}{N_{\varepsilon,i}^{M*}}\int (z - \mu_{\varepsilon,i}^{M*})^2 n_{\varepsilon,i}^{M*}(z)dz = \frac{\varepsilon\sqrt{U}}{\sqrt{s}\phi} + O(\varepsilon^2), \\ \psi_{\varepsilon,i}^{M*} = \frac{1}{N_{\varepsilon,i}^{M*}}\int (z - \mu_{\varepsilon,i}^{M*})^3 n_{\varepsilon,i}^{M*}(z)dz = O(\varepsilon^3). \end{cases} \tag{19}$$

These results are consistent with (13). Note that the equilibrium variance in each habitat $\sigma_{\varepsilon,i}^{M*2} \approx \frac{\varepsilon\sqrt{U}}{\sqrt{s}\phi}$ is larger than the equilibrium variance maintained in the absence of heterogeneity between the habitats (compare with (11)). This increase in the equilibrium variance comes from ϕ which depends on dispersion and the heterogeneity between the two habitats. The variance of the distribution increases as ϕ decreases. When $\phi = 0$ the approximation for the variance becomes infinitely large. Indeed, this corresponds to the threshold value of migration below which the above approximation collapses because the distribution becomes bimodal. In this case we have to switch to the analysis of the dimorphic case. Note that the differentiation between habitats depends also on ϕ. Some differentiation emerges even when the migration rate is above the critical migration rate, m_c (Figures 3 and 4). In Figure 4 we provide a comparison of the results from the *first* and the *second approximations*. Our *second approximation* yields convincing results when the parameters are such that we are far from the transition zone from monomorphic to dimorphic distribution. This approximation is indeed based on an integral approximation which is relevant only when the population's distribution is relatively sharp around the ESS points. This is not the case in the transition zone unless the effect of the mutations, i.e. ε, is very small.

Dimorphic case: When $m < m_c$, the only globally stable evolutionary equilibrium is dimorphic which

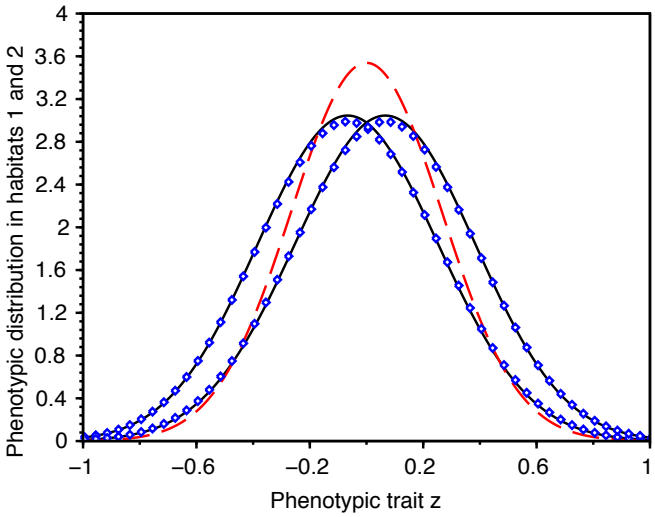

Figure 3 – Selection-mutation-migration equilibrium of the phenotypic densities $n_{\varepsilon,i}(z)$ in the two habitats in a symmetric scenario. We plot the exact phenotypic densities at equilibrium obtained from numerical computations of the equilibrium of (3) (blue dots) together with our *first approximation* (full black line) in a case where the distribution is unimodal in each habitat. We also plot the approximation given in Débarre et al. 2013 (red dashed line). Note that our approximation captures the emergence of some differentiation even though we are above the critical migration rate leading to the evolution of a dimorphic population. In the presence of large mutation rates, the population's distribution is indeed shifted to the left(respectively right) in the first(respectively second) habitat, while Débarre et al. 2013 provided the same approximation for both habitats. Our calculation yields also better approximations for the variance of the distribution in each habitat (Débarre et al. 2013 underestimates this variance). In this figure and in the following ones, to compute numerically the equilibrium, we have solved numerically the dynamic problem (3) and kept the solution obtained after long time when the equilibrium has been reached. Parameter values: $m = 1.5$, $r_{\max} = 3$, $s = 2$; $\theta = 0.5$, $\kappa = 1$, $U = 1$, $\varepsilon = 0.1$.

yields the following ESS: $\{z_{\mathrm{I}}^{D*},\ z_{\mathrm{II}}^{D*}\}$ with $z_{\mathrm{I}}^{D*} = -z_{\mathrm{II}}^{D*} = -z^{D*}$ and $z^{D*} = \frac{\sqrt{4s^2\theta^4 - m^2}}{2s\theta}$. When $\varepsilon = 0$ this yields the following phenotypic densities at equilibrium : $n_i^{D*}(z) = \nu_{\mathrm{I},i}\delta(z - z_{\mathrm{I}}^{D*}) + \nu_{\mathrm{II},i}\ \delta(z - z_{\mathrm{II}}^{D*})$ (analytic expressions for $\nu_{\mathrm{I},j}$ and $\nu_{\mathrm{II},j}$ are given in the supplementary information, Section B.1). When $\varepsilon > 0$ we can use our *first* and *second approximations* to obtain convincing approximations of the phenotypic distribution and its moments (see Figure 4). Our *first approximation* improves the Adaptive Dynamics predictions in a broad range of the parameter space and, as pointed above, our *second approximation* is pertinent when the parameters are such that we are far from the transition zone from dimorphic to monomorphic distribution. The analytic expressions for the local moments of the stationary distribution in each habitat, obtained from our *second approximation*, are given in the supplementary information, Section B.3.

Non-symmetric scenarios

A general non-symmetric scenario: In a non-symmetric scenario, there is also a unique glob-

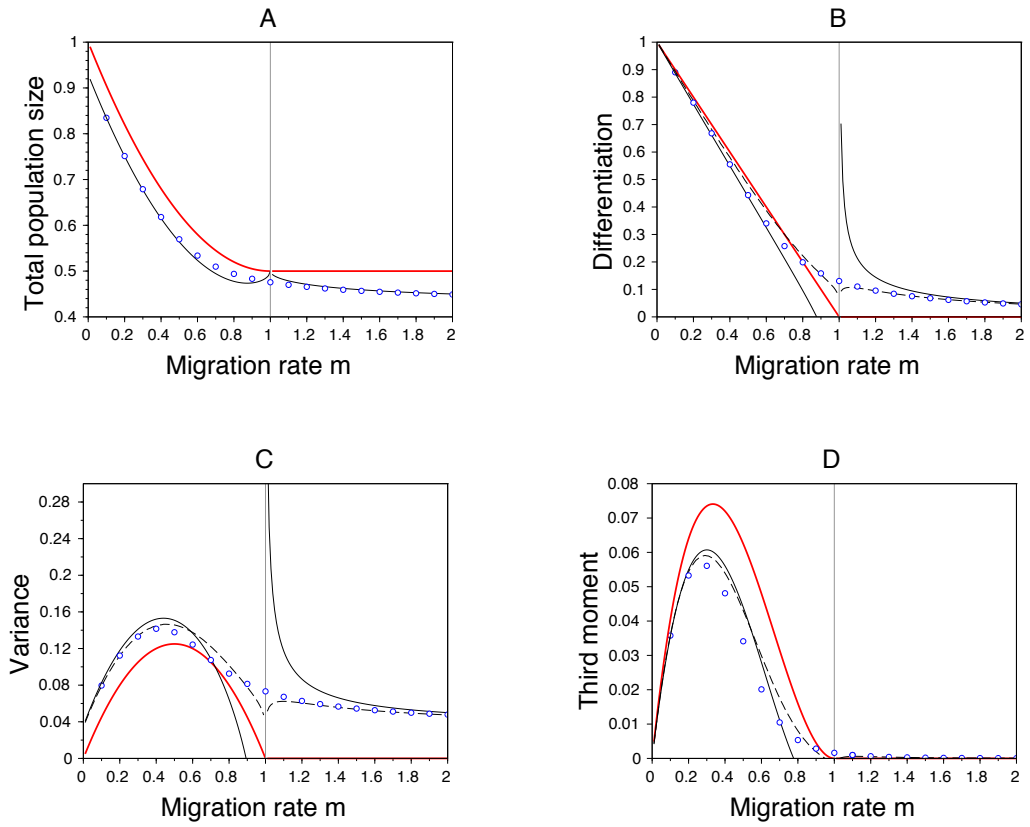

Figure 4 – Effects of migration in a symmetric scenario on (A) the total population size ($N^*_{\varepsilon,1}$) in habitat 1, (B) the differentiation between habitats ($\mu^*_{\varepsilon,2} - \mu^*_{\varepsilon,1}$), (C) the variance ($\sigma^{*2}_{\varepsilon,1}$) and (D) the third central moment of the phenotypic distribution ($\psi^*_{\varepsilon,1}$) in habitat 1 (see (19) and Section B.3 for the definition of these quantities and the analytic formula obtained from our *second approximation*). The dots refer to the numerical resolutions of the problem with $\varepsilon = 0.05$, the red line indicates the case where $\varepsilon = 0$, while the lines in black refer to our two approximations when $\varepsilon = 0.05$ (the dashed line for the *first approximation* and the full line for the *second approximation*). The vertical gray line indicates the critical migration rate below which dimorphism can evolve in the Adaptive Dynamics scenario. Note that both approximations predict the same total population size. Other parameter values: $r_{\max} = 1$, $s = 2$, $\theta = 0.5$, $\kappa = 1$, $U = 1$.

ally stable evolutionary strategy which is either monomorphic or dimorphic. There is still a threshold value of migration above which the maintenance of a dimorphic polymorphism is impossible: $\Delta = \frac{m_1 m_2}{4 s_1 s_2 \theta^4} \geq 1$. Note that this condition generalizes the condition in the symmetric case (i.e. when $m_1 = m_2$ and $s_1 = s_2$). However, for the ESS to be dimorphic, the condition $\Delta < 1$ is not enough and two other conditions should also be satisfied. These conditions (i.e. $\eta_1 < \beta_2 r_{\max,2} - \alpha_1 r_{\max,1}$ and $\eta_2 < \beta_1 r_{\max,1} - \alpha_2 r_{\max,2}$ with the constants α_i,β_i and η_i depending on the parameters m_1, m_2, s_1, s_2, κ_1, κ_2 and θ, see the supplementary information, Section B.2), guarantee that the qualities of the habitats are not very different. Indeed, if one habitat has a higher quality it is likely to overwhelm the dynamics of adaptation in the other habitat. This will yield a monomorphic equilibrium biased

toward the high-quality habitat. Figure 5 illustrates that a polymorphism is only maintained in a range of parameter values where the two habitats are relatively similar. Interestingly, in spite of the asymmetry of the two habitats, the locations of the two peaks of the phenotypic distribution are always symmetric and consequently: $z_1^{D*} = -z_2^{D*} = -z^{D*}$ where: $z^{D*} = \sqrt{\theta^2(1-\Delta)}$. The symmetric locations of the peaks is indeed a consequence of the choice of the quadratic stabilizing selection (1). See the supplementary information, Section B.1 for the expressions of the densities in each habitat and Section A.2.1.1 for the conditions leading to this stable equilibrium.

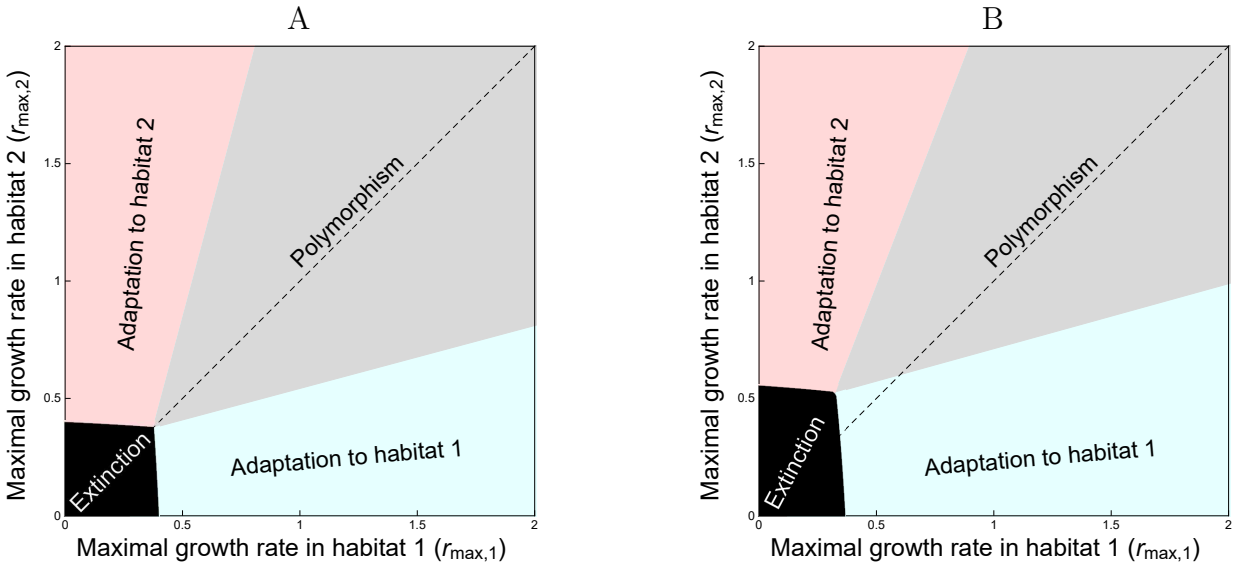

Figure 5 – Maintenance of polymorphism and non-symmetric adaptation as a function of the maximal growth rates $r_{max,1}$ and $r_{max,2}$ in the two habitats. In (A) we examine a symmetric situation where all the parameters are identical in the two habitats: $m_1 = m_2 = 0.5$, $s_1 = s_2 = 2$, $\kappa_1 = \kappa_2 = 1$. In (B) we show a non-symmetric case with the same parameters as in (A) except $m_1 = 0.5$ and $m_2 = 0.7$. The black area indicates the parameter space where the population is driven to extinction because the maximal growth rates are too low. In the grey area some polymorphism can be maintained in the two-habitat population as long as the difference in the maximal growth rates are not too high. When this difference reaches a threshold polymorphism cannot be maintained and the single type that is maintained is more adapted to the good-quality habitat (the habitat with the highest maximal growth rate).

A source-sink scenario: An extreme case of asymmetry occurs when one population (the source) does not receive any migrant from the second population (the sink). For instance, when $m_1 > 0$ and $m_2 = 0$ there is no immigration in habitat 1. Note that, this is a degenerate case and in particular, we are not anymore in the framework of Section 3.2.1, where the ESS was always the same in both habitats as a result of strict positivity of migration rate in both directions. Moreover, the computation of the equilibrium in presence of mutations is also slightly different because of this degeneracy (see the supplementary information Section A.2.2).

The evolutionary outcome in the first habitat is obvious because it depends only on selection acting

in habitat 1: the ESS is $-\theta$ and

$$N_1^* = \frac{r_{\max,1} - m_1}{\kappa_1}. \tag{20}$$

Moreover, the population's phenotypic density $n^*_{\varepsilon,1}$ can be computed explicitly: $n^*_{\varepsilon,1} = N^*_{\varepsilon,1} f_\varepsilon$, where $N^*_{\varepsilon,1} = \frac{r_{\max,1} - m_1 - \varepsilon\sqrt{U s_1}}{\kappa_1}$ and f_ε is the probability density of a normal distribution $\mathcal{N}(-\theta, \frac{\varepsilon\sqrt{U}}{\sqrt{s_1}})$.

In habitat 2, the evolutionary outcome results from the balance between migration from habitat 1 and local selection. Interestingly, migration has a non-monotonic effect on adaptation in the sink (See Figure 6). Indeed, Figure 6A shows that the population size in the sink is maximized for intermediate values of migration. More migration from the source has a beneficial effect on the demography of the sink but it prevents local adaptation. Yet, when migration from the source becomes very large it limits the size of the population in the source (see (20)). This limits the influence of the source on the sink and can even promote adaptation to the sink. In fact, it is worth noting that differentiation between the two habitats can actually increase with migration (Figure 6B). The level of migration from the source that prevents local adaptation in the sink is given by the condition:

$$\frac{4 s_2 \theta^2 r_{\max,2}}{\kappa_2} \leq \frac{m_1 (r_{\max,1} - m_1)}{\kappa_1}. \tag{21}$$

Indeed, when condition (21) is verified, the migration from the source overwhelms local selection and the evolutionary stable strategy in the sink is $z^* = -\theta$. In contrast, when condition (21) does not hold, the effective growth rate of the optimal trait θ in the sink habitat is high enough to compete with the trait $-\theta$ coming from the source, allowing coexistence between the two strategies. Note again that our two approximations (see supplementary information sections A.2.2.2 for the derivation of the *first approximation* and B.4 for the analytic formula for the moments of the phenotypic distribution derived from our *second approximation*) provide very good predictions for the moments of the phenotypic distribution in the sink (Figure 6).

4 Discussion

The balance between selection, migration and mutation drives the dynamics of local adaptation in heterogeneous environments. Here we present a new theoretical approach to obtain accurate approximations for the equilibrium phenotypic densities in a two-habitat environment. This analysis goes beyond the Adaptive Dynamics framework because it allows us to account for the effect of large mutation rates. This analysis does not rely on the Gaussian approximation which underlies many Quantitative Genetics models. Our analysis yields analytic approximations that help provide a good understanding of the balance between the different evolutionary forces in both *symmetric* and *non-symmetric* scenarios.

In the *symmetric* scenario we recover the classical results from Quantitative Genetics in a single population Lande 1975; Bürger 2000; Rice 2004 but expand this to spatially heterogeneous scenarios. In particular, we capture the emergence of differentiation between habitats when the migration rate decreases. When migration is strong relative to selection, the stationary phenotypic density is unimodal in each habitat but heterogeneous selection increases phenotypic variance and differentiation (see (19) and Figure 4). When migration is close to the critical migration rate m_c (see condition (18)) we observe a shift between the phenotypic distributions of the two habitats. This pattern was not

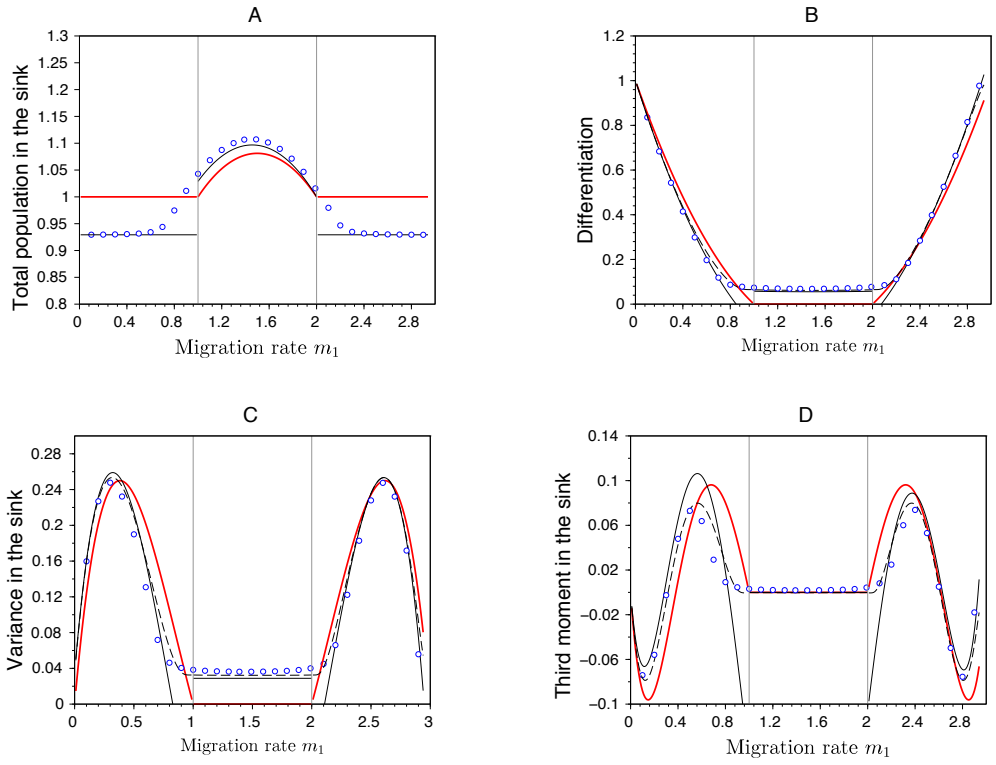

Figure 6 – Effects of migration in a source-sink scenario on (A) the total population size in the sink habitat, (B) the differentiation between habitats, (C) the variance and (D) the third central moment of the phenotypic distribution in sink. The dots refer to exact numerical computations when $\varepsilon = 0.05$, the red line indicates the case where $\varepsilon = 0$ while the lines in black refer to our two approximations when $\varepsilon = 0.05$ (dashed line for the *first approximation* and the full line for the *second approximation*). The vertical gray lines, at $m_1 = 1$ and $m_1 = 2$, indicate the critical migration rates where transition occurs between monomorphism and dimorphism in the Adaptive Dynamics framework (see condition (21)). Note that both approximations predict the same total population size. Other parameter values: $r_{\max,1} = 3$, $r_{\max,2} = 1$, $s_1 = 3$, $s_2 = 2$, $\kappa_1 = \kappa_2 = 1$, $\theta = 0.5$, $U = 1$.

detected in previous studies but our method captures this shift and improves the approximation of the variance of the phenotypic distributions (see Débarre et al. 2013 and Figure 3). When the migration rate is much smaller than m_c and selection is sufficiently strong between habitats, the equilibrium distribution in each habitat can be well approximated as the sum of two distributions. But unlike previous approximations Yeaman and Guillaume 2009; Débarre et al. 2013 these two distributions are non-gaussian. We derive approximations for the moments of these distributions. In other words, this work generalises previous attempts to derive the distribution of a phenotypic trait at the mutation-selection-migration equilibrium. Our results confirm the importance of the skewness in the phenotypic distribution and improve predictions of measures of local adaptation in a heterogeneous environment.

In the *non-symmetric* scenario we show that the condition for the maintenance of two specialized

strategies are more restrictive (Figure 5). Indeed, asymmetries promote a single strategy that is more locally adapted to the habitat with larger population size and/or lower immigration rate. The impact of biased migration rates from a source population into the adaptation of peripheral populations has been discussed before Holt and Gaines 1992; García-Ramos and Kirkpatrick 1997; Gomulkiewicz et al. 1999; Holt et al. 2003; Akerman and Bürger 2014. Our approach, however, yields a quantitative description of the shape of the phenotypic distributions in both the source and the sink habitats. These accurate predictions are key to understand the effect of different evolutionary forces on the level of adaptation in the two habitats. For instance, the analysis of an extreme case with source-sink dynamics reveals the complex interplay between migration, demography and local selection. The maintenance of a polymorphic equilibrium is possible when migration from the source is either very weak or very strong. This result challenges the classical prediction where migration is always an homogenizing force reducing the differentiation among populations (Figure 6).

Our work illustrates the potential of a new mathematical tool in the field of evolutionary biology. In this work, we use an approach based on Hamilton-Jacobi equations (see (A.22)) which has been developed, mostly by the mathematical community, during the last decade to describe the asymptotic solutions of the selection-mutation models, as the effect of mutation vanishes. We refer to Diekmann et al. 2005; Perthame and Barles 2008; Mirrahimi 2011 for the establishment of the basis of this approach. Note, however, that previous studies were mainly focused on the limit case where the effects of mutations are vanishingly small. In particular, they do not provide approximations of the phenotypic density and its moments when the effect of mutations, ε, is nonzero. In the present work we go further than the previous studies and characterize the phenotypic distributions when the influx of mutations can alter significantly the shape of the stationary distribution. Understanding the build up of this distribution is particularly important to study the effect of mutation on adaptation. Although mutation is the ultimate source of adaptive variation, the accumulation of deleterious mutations generates a load on the average fitness of populations. This is particularly relevant in organisms like RNA viruses which are characterized by very large mutation rates Drake and Holland 1999; Sanjuán et al. 2010. In fact, the mutation loads of RNA virus is so high that it may even lead some populations to extinction Bull et al. 2007; Martin and Gandon 2010. Our model can be used to accurately capture the effect of increasing mutation rates on the mutation load of a population living in a heterogeneous environment (Figure 7). This heterogeneity may be particularly relevant in chronic infections by pathogenic virus that can adapt to different organs Kemal et al. 2003; Sanjuán et al. 2004; Ducoulombier et al. 2004; Jridi et al. 2006. A better understanding of the phenotypic distribution at equilibrium in heterogeneous environments may thus provide more accurate prediction on the critical mutation rates that can ultimately lead within-host dynamics to pathogen extinction.

Our analysis of the equilibrium between selection, migration and mutation could be extended in several new directions. More than 2 habitats could be considered, or different growth rates and/or mutation kernels could be used (see Mirrahimi 2013 and the supplementary information, Section A.3). The approach could also be used to analyze situations away from the equilibrium. For instance, it would be possible to track the dynamics of the distribution as the population adapts to a new environment or to a time-varying environment Lande and Shannon 1996. Hamilton-Jacobi equations have indeed also been used to study time-varying (but space homogeneous) environments (see for instance Mirrahimi et al. 2015; Figueroa Iglesias and Mirrahimi 2018). Finally, it is interesting to note that the generalization of the present ecological scenario to model the adaptation of sexual species in heterogeneous environments remains to be carried out. Our method could be extended to allow for sexual

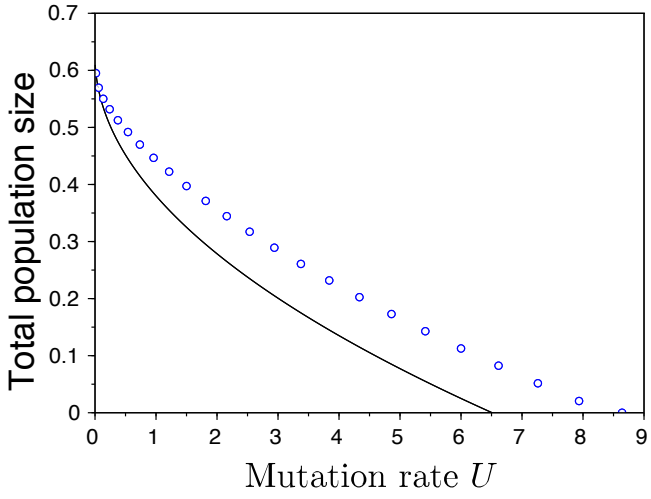

Figure 7 – Effect of increasing the mutation rate U on the total population size in the symmetric scenario used in Figure 3 with $m = 0.5$. The full line indicates the approximation and the dots are the results of exact numerical computations. This figure illustrates that our approximation given by the first line of (19) captures reasonably well the effect of large mutation rates on the mutation load in a two-habitat scenario where there is differentiation and some local adaptation.

reproduction within the framework of the infinitesimal model (see Fisher 1919; Calvez et al. 2019). But this analysis falls beyond the scope of the present paper.

Acknowledgements

The first author is grateful for partial funding from the European Research Council (ERC) under the European Union's Horizon 2020 research and innovation programme (grant agreement No 639638), held by Vincent Calvez, and from the french ANR projects KIBORD ANR-13-BS01-0004 and MODEVOL ANR-13-JS01-0009.

References

Akerman, A. and Bürger, R. (2014). The consequences of gene flow for local adaptation and differentiation: a two-locus two-deme model. *Journal of Mathematical Biology*, 68(5):1135–1198.

Barles, G., Mirrahimi, S., and Perthame, B. (2009). Concentration in Lotka-Volterra parabolic or integral equations: a general convergence result. *Methods Appl. Anal.*, 16(3):321–340.

Bull, J. J., Sanjuan, R., and Wilke, C. O. (2007). Theory of lethal mutagenesis for viruses. *Journal of virology*, 81(6):2930–2939.

Bürger, R. (2000). *The Mathematical theory of selection, recombination and mutation*. Wiley, New-York.

Calvez, V., Garnier, J. and Patout, F. (2019) A quantitative genetics model with sexual mode of reproduction in the regime of small variance. *Preprint arXiv:1811.01779*.

Caswell, H. (1989). *Matrix Population Models*. Sinauer Associates.

Champagnat, N., Ferrière, R., and Méléard, S. (2008). *Individual-based probabilistic models of adaptive evolution and various scaling approximations*, volume 59 of *Progress in Probability*, pages 75–114. Birkhäuser.

Christiansen, F. B. (1975). Hard and soft selection in a subdivided population. *The American Naturalist*, 109(965):11–16.

Day, T. (2000). Competition and the effect of spatial resource heterogeneity on evolutionary diversification. *The American Naturalist*, 155(6):790–803.

Débarre, F. and Gandon, S. (2010). Evolution of specialization in a spatially continuous environment. *Journal of Evolutionary Biology*, 23(5):1090–1099.

Débarre, F., Ronce, O., and Gandon, S. (2013). Quantifying the effects of migration and mutation on adaptation and demography in spatially heterogeneous environments. *Journal of Evolutionary Biology*, 26:1185–1202.

Débarre, F., Yeaman, S., and Guillaume, F. (2015). Evolution of quantitative traits under a migration-selection balance: when does skew matter? *The American Naturalist*, 186(37–47).

Diekmann, O., Jabin, P.-E., Mischler, S., and Perthame, B. (2005). The dynamics of adaptation: an illuminating example and a Hamilton-Jacobi approach. *Th. Pop. Biol.*, 67(4):257–271.

Doebeli, M. and Dieckmann, U. (2003). Speciation along environmental gradients. *Nature*, 421:259–264.

Drake, J. W. and Holland, J. (1999). Mutation rates among rna viruses. *Proceedings of the National Academy of Sciences of the United States of America*, 96(24):13910–3.

Ducoulombier, D., Roque-Afonso, A.-M., Di Liberto, G., Penin, F., Kara, R., Richard, Y., Dussaix, E., and Féray, C. (2004). Frequent compartmentalization of hepatitis c virus variants in circulating b cells and monocytes. *Hepatology*, 39(3):817–825.

Fabre, C., Méléard, S., Porcher, E., Teplitsky, C., and A., R. (2012) Evolution of a structured population in a heterogeneous environment. *Preprint*.

Figueroa Iglesias, S. and Mirrahimi, S. (2018). Long time evolutionary dynamics of phenotypically structured populations in fluctuating environments. *SIAM J. Math. Anal.*, 50(5):5537–5568.

Fisher, R. A. (1919) Xv.-the correlation between relatives on the supposition of mendelian inheritance. *Earth and Environmental Science Transactions of the Royal Society of Edinburgh*, 52(2):399–433.

Gandon, S. and Mirrahimi, S. (2016) A Hamilton-Jacobi method to describe the evolutionary equilibria in heterogeneous environments and with non-vanishing effects of mutations. *Comptes Rendus - Mathematique*, 355(2):155–160.

García-Ramos, G. and Kirkpatrick, M. (1997). Genetic models of adaptation and gene flow in peripheral populations. *Evolution*, 51(1):21–28.

Geritz, S. A. H., Kisdi, E., Mészena, G., and Metz, J. A. J. (1998). Evolutionarily singular strategies and the adaptive growth and branching of the evolutionary tree. *Evol. Ecol*, 12:35–57.

Gomulkiewicz, R., Holt, R. D., and Barfield, M. (1999). The effects of density dependence and immigration on local adaptation and niche evolution in a black-hole sink environment. *Theoretical population biology*, 55(3):283–296.

Holt, R. D. and Gaines, M. S. (1992). Analysis of adaptation in heterogeneous landscapes: implications for the evolution of fundamental niches. *Evolutionary Ecology*, 6(5):433–447.

Holt, R. D., Gomulkiewicz, R., and Barfield, M. (2003). The phenomenology of niche evolution via quantitative traits in a 'black-hole' sink. *Proceedings of the Royal Society of London B: Biological Sciences*, 270(1511):215–224.

Jridi, C., Martin, J.-F., Marie-Jeanne, V., Labonne, G., and Blanc, S. (2006). Distinct viral populations differentiate and evolve independently in a single perennial host plant. *Journal of Virology*, 80(5):2349–2357.

Kemal, K. S., Foley, B., Burger, H., Anastos, K., Minkoff, H., Kitchen, C., Philpott, S. M., Gao, W., Robison, E., Holman, S., et al. (2003). Hiv-1 in genital tract and plasma of women: compartmentalization of viral sequences, coreceptor usage, and glycosylation. *Proceedings of the National Academy of Sciences*, 100(22):12972–12977.

Kimura, M. (1965). A stochastic model concerning the maintenance of genetic variability in quantitative characters. *Proc. Natl. Acad. Sci. USA*, 54:731–736.

Kingman, J. F. C. (1978). A simple model for the balance between selection and mutation. *J. Appl. Prob.*, 15:1–12.

Lande, R. (1975). The maintenance of genetic variability by mutation in a polygenic character with linked loci. *Genetical Research*, 26(3):221?235.

Lande, R. and Shannon, S. (1996). The role of genetic variation in adaptation and population persistence in a changing environment. *Evolution*, 50(1):434–437.

Leimar, O., Doebeli, M., and Dieckmann, U. (2008). Evolution of phenotypic clusters through competition and local adaptation along an environmental gradient. *Evolution*, 62(4):807–822.

Lenormand, T. (2002). Gene flow and the limits to natural selection. *Trends Ecol Evol*, 17(4):183–189.

Martin, G. and Gandon, S. (2010). Lethal mutagenesis and evolutionary epidemiology. *Philosophical Transactions of the Royal Society of London B: Biological Sciences*, 365(1548):1953–1963.

Meszéna, G., Czibula, I., and Geritz, S. (1997). Adaptive dynamics in a 2-patch environment: a toy model for allopatric and parapatric speciation. *Journal of Biological Systems*, 5(02):265–284.

Metz, J.A.J. and Nisbet , R. M. and Geritz, S. A. H. (1992) How should we define 'fitness' for general ecological scenarios? *Trends Ecol Evol* , 7(6):198–202.

Mirrahimi, S. (2011). *Concentration phenomena in PDEs from biology.* PhD thesis, Univeristy of Pierre et Marie Curie (Paris 6).

Mirrahimi, S. (2013). Migration and adaptation of a population between patches. *Discrete and Continuous Dynamical Systems - Series B (DCDS-B)*, 18(3):753–768.

Mirrahimi, S. (2017). A Hamilton-Jacobi approach to characterize the evolutionary equilibria in heterogeneous environments. *Math. Models Methods Appl. Sci.*, 27(13):2425–2460.

Mirrahimi, S., Perthame, B., and Souganidis, P. E. (2015). Time fluctuations in a population model of adaptive dynamics. *Annales de l'Institut Henri Poincare (C) Analyse Non Linéaire*, 32(1):41–58.

Nagylaki, T. (1978). A diffusion model for geographically structured populations. *Journal of Mathematical Biology*, 6(4):375–382.

Perthame, B. and Barles, G. (2008). Dirac concentrations in Lotka-Volterra parabolic PDEs. *Indiana Univ. Math. J.*, 57(7):3275–3301.

Rice, S. H. (2004). *Evolutionary theory: mathematical and conceptual foundations.* Sinauer Associates, Inc.

Ronce, O. and Kirkpatrick, M. (2001). When sources become sinks: migration meltdown in heterogeneous habitats. *Evolution*, 55(8):1520–1531.

Sanjuán, R., Codoñer, F. M., Moya, A., and Elena, S. F. (2004). Natural selection and the organ-specific differentiation of hiv-1 v3 hypervariable region. *Evolution*, 58(6):1185–1194.

Sanjuán, R., Nebot, M., Chirico, N., Mansky, L., and Belshaw, R. (2010). Viral mutation rates. *Journal of Virology*, 84(19):9733–9748.

Savolainen, O., Lascoux, M., and Merilä, J. (2013). Ecological genomics of local adaptation. *Nature Reviews Genetics*, 14:807–820.

Slatkin, M. (1978). Spatial patterns in the distributions of polygenic characters. *Journal of Theoretical Biology*, 70(2):213 – 228.

Szilágyi, A. and Meszéna, G. (2009). Two-patch model of spatial niche segregation. *Evolutionary Ecology*, 23(2):187–205.

Turelli, M. (1984). Heritable genetic variation via mutation-selection balance: Lerch's zeta meets the abdominal bristle. *Theoretical Population Biology*, 25(2):138 – 193.

Whitlock, M. C. (2015). Modern approaches to local adaptation. *The American Naturalist*, 186(S1):S1–S4. PMID: 26098334.

Yeaman, S. and Guillaume, F. (2009). Predicting adaptation under migration load: the role of genetic skew. *Evolution*, 63(11):2926–2938.

Part

Supporting Information

Supporting Information

Table of Contents

A Mathematical derivation

In this section, we provide the mathematical derivation of our results. In Section A.1 we treat the case of one habitat. In Section A.2 we provide our derivations for the case of two habitats. Finally in Section A.3 we show how our method can be used to study model (2).

A.1 One population

A.1.1 Derivation of our *first approximation* in absence of migration

Our *first approximation* is based on the computation of the terms $u_0(z)$ and $v_0(z)$. Based on such computations we can provide an approximation of the population's total density $N^*_{\varepsilon,0}$ and the phenotypic density $n^*_{\varepsilon,0}(z)$ in the following form

$$N^*_{\varepsilon,0} \approx N_0 + \varepsilon K_0, \qquad n^*_{\varepsilon,0}(z) \approx \frac{1}{\sqrt{2\pi\varepsilon}} \exp\big(\frac{u_0(z) + \varepsilon v_0(z)}{\varepsilon}\big). \tag{A.1}$$

Indeed we neglect the error term in (9) since when ε is small, in view of (7), it has only small contribution to the phenotypic density $n^*_{\varepsilon,0}(z)$.
We will prove in what follows that $N_0 = N_0^*$, with N_0^* the total population size at the demographic equilibrium of the ESS z_0. We will also compute the other terms of the expansions K_0, $u_0(z)$ and $v_0(z)$.
Using (5) and $\varepsilon = \sqrt{V_m}$, the equilibrium $n^*_{\varepsilon,0}(z)$ solves:

$$0 = U\varepsilon^2 \frac{\partial^2 n^*_{\varepsilon,0}(z)}{\partial z^2} + n^*_{\varepsilon,0}(z)\left(r_0(z) - \kappa_0 N^*_{\varepsilon,0}\right). \tag{A.2}$$

Replacing (7) in the above equation we obtain:

$$0 = U\varepsilon \frac{\partial^2 u_{\varepsilon,0}(z)}{\partial z^2} + U|\frac{\partial}{\partial z} u_{\varepsilon,0}(z)|^2 + r_0(z) - \kappa_0 N^*_{\varepsilon,0}. \tag{A.3}$$

This equation is derived using the following equalities:

$$\frac{\partial}{\partial z} n^*_{\varepsilon,0}(z) = \big(\frac{\partial}{\partial z} u_{\varepsilon,0}(z)\big) \frac{n^*_{\varepsilon,0}(z)}{\varepsilon}, \qquad \frac{\partial^2}{\partial z^2} n^*_{\varepsilon,0}(z) = \left(\varepsilon \frac{\partial^2}{\partial z^2} u_{\varepsilon,0}(z) + |\frac{\partial}{\partial z} u_{\varepsilon,0}(z)|^2\right) \frac{n^*_{\varepsilon,0}(z)}{\varepsilon^2}.$$

We then replace the ansatz (9) in (A.3). We first keep the zero order terms with respect to ε (the ones in front of which there is no ε, corresponding to the dominant terms) to obtain the following equation on $u_0(z)$:

$$0 = U|\partial_z u_0(z)|^2 + r_0(z) - \kappa_0 N_0.$$

Note also that to have a finite but positive size of population, we should have

$$\max_{z\in\mathbb{R}} u_0(z) = 0.$$

Otherwise, in view of (7), the total population size whether becomes infinite as $\varepsilon \to 0$ (if $\max_{z\in\mathbb{R}} u_0(z) > 0$) or it goes to 0 (if $\max_{z\in\mathbb{R}} u_0(z) < 0$).

At the maximum point $z_{\max}$ of u_0, we have $\partial_z u_0(z_{\max}) = 0$ and hence

$$r_0(z_{\max}) - \kappa_0 N_0 = 0.$$

For all other traits z

$$r_0(z) - \kappa_0 N_0 = -U|\partial_z u_0(z)|^2 \leq 0.$$

We deduce that $z_{\max}$ is the maximum point of $r_0(z)$, that is $z_{\max} = z_0$. In other words, u takes its maximum at the ESS point z_0 and the zero order term N_0 in the approximation of the population size is given by

$$N_0 = \frac{r_0(z_0)}{\kappa_0}. \tag{A.4}$$

This corresponds indeed to the total population size N_0^* at the demographic equilibrium of the ESS z_0. We gather our results on u_0 in the following form Perthame and Barles 2008; Barles et al. 2009: u_0 is indeed the unique solution to the following Hamilton-Jacobi equation

$$\begin{cases} 0 = U|\partial_z u_0(z)|^2 + w(z; N_0^*), \\ \max_z u_0(z) = u_0(z_0) = 0, \end{cases} \tag{A.5}$$

where we recall that $w(z; N_0^*) = r_0(z) - \kappa_0 N_0^*$. This equation can be solved explicitly. The solution $u_0(z)$ is given by

$$u_0(z) = -\frac{1}{\sqrt{U}} \Big| \int_{z_0}^{z} \sqrt{-w(y, N_0^*)} dy \Big|. \tag{A.6}$$

The reader can verify that $u_0(z)$, given by the formula above, is smooth and solves (A.5). Note that the absolute values are necessary since the upper limit of the integral z can be smaller or larger than the lower limit z_0.
We then keep the terms of order ε

$$-U \frac{\partial^2}{\partial z^2} u_0(z) = 2U \frac{\partial}{\partial z} v_0(z) \frac{\partial}{\partial z} u_0(z) - \kappa_0 K_0. \tag{A.7}$$

An evaluation of this equation at the point z_0 gives

$$K_0 = \frac{U}{\kappa_0} \frac{\partial^2}{\partial z^2} u_0(z_0). \tag{A.8}$$

The function $v_0(z)$ can also be computed thanks to (A.7), that is by integrating the following quantity

$$\frac{\partial}{\partial z} v_0(z) = \frac{-U \frac{\partial^2}{\partial z^2} u_0(z) + \kappa_0 K_0}{2U \frac{\partial}{\partial z} u_0(z)}. \tag{A.9}$$

Note that to compute $v_0(z)$ we also need to choose the value of $v_0(z_0)$. This value is fixed in a way such that

$$\int_{-\infty}^{\infty} \frac{1}{\sqrt{2\pi\varepsilon}} \exp\big(\frac{u_0(z) + \varepsilon v_0(z)}{\varepsilon}\big) dz = N_0^* + \varepsilon K_0. \tag{A.10}$$

Example of quadratic growth rate (10)**.** In this example the ESS, which is indeed the maximum

point of $r_0(z)$, is given by $z_0 = \theta_0$. Considering the specific fitness function (10) in (A.4) we first obtain that

$$N_0^* = \frac{r_{\max,0}}{\kappa_0}.$$

Using (A.6) we then obtain that

$$u_0(z) = -\frac{1}{\sqrt{U}}\Big|\int_{\theta_0}^{z}\sqrt{s_0(y-\theta_0)^2}dy\Big| = -\frac{\sqrt{s_0}}{2\sqrt{U}}(z-\theta_0)^2.$$

We also obtain from (A.8) that $K_0 = -\frac{\sqrt{s_0 U}}{\kappa_0}$. Moreover, from (A.9) we obtain that $\frac{\partial}{\partial z}v_0(z) = 0$ which means that $v_0(z)$ is a constant. Combining these informations with (A.10) we obtain

$$N^*_{\varepsilon,0} \approx \frac{1}{\kappa_0}(r_{\max,0} - \varepsilon\sqrt{s_0 U}), \quad n^*_{\varepsilon,0}(z) \approx \frac{1}{\sqrt{2\pi\varepsilon}}\exp\big(\frac{u_0(z)+\varepsilon v_0(z)}{\varepsilon}\big) = \frac{N^*_{\varepsilon,0}s_0^{1/4}}{\sqrt{2\pi\varepsilon\sqrt{U}}}\exp\big(-\frac{\sqrt{s_0}}{2\varepsilon\sqrt{U}}(z-\theta_0)^2\big).$$

In other words, our *first approximation* of the phenotypic density $n^*_{\varepsilon,0}(z)$ is given by (8) and (11). We note finally that the Gaussian distribution obtained above solves (A.2) and hence it is indeed an exact solution.

Example of non-symmetric growth rate (12)**.** In this example similarly to the previous example the ESS z_0 is given by $z_0 = \theta_0$ and

$$N_0^* = \frac{r_{\max,0}}{\kappa_0}.$$

The expression of $u_0(z)$ is however different, and it is given thanks to (A.6) by

$$u_0(z) = -\frac{1}{\sqrt{U}}\Big|\int_{\theta_0}^{z}\sqrt{s_0(y-\theta_0)^2(a+(y-\theta_0-b)^2)}dy\Big|. \tag{A.11}$$

From this expression we can then compute K_0 and $v_0(z)$ similarly to above using (A.8) and (A.9).

A.1.2 Derivation of our *second approximation* in absence of migration

In this section, we provide the main idea to obtain explicit formula for the moments of the population's distribution. The computation of explicit formula for the moments of the population's distribution is based on the observation that, when ε is small, the phenotypic density $n^*_{\varepsilon,0}(z)$ is exponentially small far from the ESS point, since $u_0(z)$ takes negative values at those points. Therefore, only the values of $u_0(z)$ and $v_0(z)$ around the ESS point matter. We indeed use the Taylor expansions of $u_0(z)$ and $v_0(z)$ around the ESS point to compute such analytic formula.
We first provide our analytic formula for the moments of the population's distribution. We next show how to compute such approximations.

Analytic formula for the moments of the population's distribution. According to Section 3.1.1 there exists a unique ESS which is monomorphic and given by z_0. In order to provide an explicit approximation of the moments of the population's distribution, we compute the third order approximation of $u_0(z)$ around z_0:

$$u_0(z) = -\frac{A}{2}(z-z_0)^2 + B(z-z_0)^3 + O(z-z_0)^4, \tag{A.12}$$

and the first order approximation of $v_0(z)$ around z_0:

$$v_0(z) = \log(\sqrt{A}N_0^*) + D(z - z_0) + O(z - z_0)^2. \tag{A.13}$$

Such coefficients can be computed thanks to (A.6) and (A.9). To obtain the zero order term in the expansion for $v_0(z)$ we use the fact that, as the mutation's variance vanishes ($\varepsilon \to 0$), the total population size $N^*_{\varepsilon,0}$ tends to N_0^* which corresponds to the demographic equilibrium at the ESS.
The above approximation allows us to estimate the moments of the population's distribution:

$$\begin{cases} \mu^*_{\varepsilon,0} = \frac{1}{N^*_{\varepsilon,0}} \int z n^*_{\varepsilon,0}(z)dz = z_0 + \varepsilon(\frac{3B}{A^2} + \frac{D}{A}) + O(\varepsilon^2), \\ \sigma^{*\,2}_{\varepsilon,0} = \frac{1}{N^*_{\varepsilon,0}} \int (z - \mu^*_{\varepsilon,0})^2 n^*_{\varepsilon,0}(z)dz = \frac{\varepsilon}{A} + O(\varepsilon^2), \\ \psi^*_{\varepsilon,0} = \frac{1}{N^*_{\varepsilon,0}} \int (z - \mu^*_{\varepsilon,0})^3 n^*_{\varepsilon,0}(z)dz = \frac{6B}{A^3}\varepsilon^2 + O(\varepsilon^3). \end{cases} \tag{A.14}$$

Derivation of the analytic formula. We next show how to compute such approximations. We can indeed use the expressions in (A.12) and (A.13) to compute for any integer $k \geq 1$,

$$\begin{aligned} \int (z - z_0)^k n^*_{\varepsilon,0}(z)dz &= \frac{\varepsilon^{\frac{k}{2}}\sqrt{A}N_0^*}{\sqrt{2\pi}} \int_{\mathbb{R}} (y^k e^{-\frac{A}{2}y^2}\big(1 + \sqrt{\varepsilon}(By^3 + Dy) + O(\varepsilon)\big)dy \\ &= \varepsilon^{\frac{k}{2}} N_0^* \Big(\omega_k(\tfrac{1}{A}) + \sqrt{\varepsilon}\big(B\omega_{k+3}(\tfrac{1}{A}) + D\omega_{k+1}(\tfrac{1}{A})\big)\Big) + O(\varepsilon^{\frac{k+2}{2}}), \end{aligned}$$

where $\omega_k(\sigma^2)$ corresponds to the k-th order central moment of a Gaussian distribution with variance σ^2. Note that to compute the integral terms above we have performed a change of variable $z - z_0 = \sqrt{\varepsilon}y$, therefore each term $z - z_0$ can be considered as of order $\sqrt{\varepsilon}$ in the integrations. Note also that since the term v is multiplied by ε in (9), a first order expansion of v is enough, while a third order expansion of u is required to obtain the above approximation. The above integrations are the main ingredients to obtain the approximations given in (A.14), i.e. our *second approximation*.

Example of non-symmetric growth rate (12)**.** Using (A.11) and (A.9) we can compute the coefficients in the Taylor expansions of $u_0(z)$ and $v_0(z)$, that is (A.12) and (A.13), to obtain

$$A = \frac{\sqrt{s_0(a + b^2)}}{\sqrt{U}}, \quad B = \frac{\sqrt{s_0}\, b}{3\sqrt{U(a + b^2)}}, \qquad D = \frac{b}{a + b^2}.$$

Then the expressions of $\mu^*_{\varepsilon,0}$, $\sigma^{*2}_{\varepsilon,0}$ and $\psi^*_{\varepsilon,0}$ at the end of Section 3.1.2 can be derived thanks to (A.14).

A.2 Two populations

This section is devoted to the mathematical derivation of our results in the case of two habitats. In Subsection A.2.1 we provide the mathematical derivation of our result in the general case. In Subsection A.2.2 we treat the extreme case where there is no migration from habitat 2, that is $m_2 = 0$.

A.2.1 A general case (where $m_1 > 0$ and $m_2 > 0$)

In Subsection A.2.1.1, we provide the details of our results in the Adaptive Dynamics framework. In Subsection A.2.1.2 we present the analysis to obtain our *first approximation*. In Subsection A.2.1.3 we provide the derivation of our *second approximation*.

A.2.1.1 Adaptive dynamics in presence of migration In this section, we provide the conditions for a global evolutionary stable strategy. To be able to characterize the ESS one should first characterize the demographic equilibrium corresponding to a set of traits. Because there are only two habitats, at most two distinct traits can co-exist. Therefore, we only need to consider two scenarios where the phenotypic distribution is either monomorphic (with phenotype z^M) or dimorphic (with phenotypes $z^D_{\rm I}$ and $z^D_{\rm II}$, where the subscripts I and II indicate that the phenotype is best adapted to habitat 1 and 2, respectively).

The monomorphic equilibrium is given by $n_i^M(z) = N_i^M \delta(z - z^M)$ where $\delta(.)$ is the dirac delta function, $\left(N_1^M, N_2^M\right)^T$ is the right eigenvector associated with the dominant eigenvalue $W(z^M; N_1^M, N_2^M) = 0$ of $\mathcal{A}(z^M; N_1^M, N_2^M)$. In a similar way the dimorphic equilibrium is characterized by: $n_i^D(z) = \nu_{\rm I,i}\delta(z - z^D_{\rm I}) + \nu_{\rm II,i}\delta(z - z^D_{\rm II})$, where $\nu_{\rm I,i} + \nu_{\rm II,i} = N_i^D$ and $(\nu_{k,1}, \nu_{k,2})^T$ are the right eigenvectors associated with the largest eigenvalues $W(z_k^D; N_1^D, N_2^D) = 0$ (for $k = {\rm I}, {\rm II}$) of $\mathcal{A}(z_k^D; N_1^D, N_2^D)$.

The evolutionary stability of a resident strategy z^{M*} can be studied with the analysis of the invasion of a new mutant strategy z_m at the demographic equilibrium $\left(N_1^{M*}, N_2^{M*}\right)$ set by the resident strategy. The monomorphic strategy z^{M*} is an evolutionary stable strategy if for any mutant $z_m \neq z^{M*}$, the effective fitness is negative: $W(z_m; N_1^{M*}, N_2^{M*}) < 0$. In a similar way, the dimorphic strategy $\{z^{D*}_{\rm I}, z^{D*}_{\rm II}\}$ is an evolutionary stable strategy if for any mutant $z_m \notin \{z^{D*}_{\rm I}, z^{D*}_{\rm II}\}$, the effective fitness is negative: $W(z_m; N_1^{D*}, N_2^{D*}) < 0$.

To determine the global ESS, we first define

$$z^{D*} = \sqrt{\theta^2 - \frac{m_1 m_2}{4\theta^2 s_1 s_2}}, \qquad N_1^{D*} = \frac{\frac{m_1 m_2}{4\theta^2 s_2} + r_{\max,1} - m_1}{\kappa_1}, \qquad N_2^{D*} = \frac{\frac{m_1 m_2}{4\theta^2 s_1} + r_{\max,2} - m_2}{\kappa_2}.$$

Theorem A.1 *Mirrahimi 2017 There exists a unique global ESS.*
(i) The ESS is dimorphic if

$$\frac{m_1 m_2}{4 s_1 s_2 \theta^4} < 1, \tag{A.15}$$

$$0 < m_2 N_2^{D*} + (w_1(-z^{D*}; N_1^{D*}) - m_1) N_1^{D*}, \tag{A.16}$$

and

$$0 < m_1 N_1^{D*} + (w_2(z^{D*}; N_2^{D*}) - m_2) N_2^{D*}. \tag{A.17}$$

Then the dimorphic equilibrium is given by

$$n_i^{D*} = \nu_{{\rm I},i}\delta(z + z^{D*}) + \nu_{{\rm II},i}\delta(z - z^{D*}), \quad \nu_{{\rm I},i} + \nu_{{\rm II},i} = N_i^{D*}, \quad i = 1, 2,$$

with $\nu_{k,i}$ given in Section B.1.
(ii) If the above conditions are not satisfied then the ESS is monomorphic. In the case where condition (A.15) *is verified but the r.h.s. of* (A.16) *(respectively* (A.17)*) is negative, the fittest trait belongs to*

the interval $(-\theta, -z^{D*})$ *(respectively* (z^{D*}, θ)*). If* (A.15) *is satisfied but* (A.16) *(respectively* (A.17)*) is an equality then the monomorphic ESS is given by* $\{-z^{D*}\}$ *(respectively* $\{z^{D*}\}$*).*

If the habitats are symmetric, then the second and the third conditions (A.16)–(A.17) above are always satisfied and the dimorphism occurs under the only condition (A.15). In other words, if migration is weak with respect to the selection or the difference of the optimal traits in the two habitats, then the ESS will be dimorphic. When the habitats are non-symmetric the extra conditions (A.16) and (A.17) appear which are conditions of mutual invasibility. Condition (A.16) (respectively condition (A.17)) means indeed that a mutant trait of type z^{D*} (respectively $-z^{D*}$) can invade a monomorphic resident population of type $-z^{D*}$ (respectively z^{D*}) which is at it's demographic equilibrium (see Mirrahimi 2017-Proposition 3.4).
We can indeed rewrite conditions (A.16) and (A.17) respectively as below

$$\eta_1 \, < \, \beta_2 r_{\max,2} - \alpha_1 r_{\max,1}, \qquad \eta_2 \, < \, \beta_1 r_{\max,1} - \alpha_2 r_{\max,2},$$

with η_i, α_i and β_i constants depending on m_1, m_2, g_1, g_2, κ_1, κ_2 and θ (see Section B.2 for the expressions of these coefficients). These conditions, which are given in Section 3.2.3 in the general non-symmetric scenario, are indeed a measure of asymmetry between the habitats. They appear from the fact that even if condition (A.15), which is the only condition for dimorphism in symmetric habitats, is satisfied, while the quality of the habitats are very different, the ESS cannot be dimorphic. In this case, the population will be able to adapt only to one of the habitats and it will be maladapted to the other one (see Figure 5). To avoid lengthy and technical computations, the proof of Theorem (A.1) is given in Mirrahimi 2017–Section 4.

A.2.1.2 Derivation of our *first approximation* in presence of migration Similarly to Subsection A.1.1 our *first approximation* is based on the computation of the terms $u_i(z)$ and $v_i(z)$. Based on such computations we can provide an approximation of the population's total density $N^*_{\varepsilon,i}$ and the phenotypic density $n^*_{\varepsilon,i}(z)$ in the following form

$$N^*_{\varepsilon,i} \approx N_i + \varepsilon K_i, \qquad n^*_{\varepsilon,i}(z) \propto \frac{1}{\sqrt{2\pi\varepsilon}} \exp\big(\frac{u_i(z) + \varepsilon v_i(z)}{\varepsilon}\big). \tag{A.18}$$

Note that the equilibrium $(n^*_{\varepsilon,1}, n^*_{\varepsilon,2})$ solves

$$\begin{cases} 0 = U\varepsilon^2 \frac{\partial^2 n^*_{\varepsilon,1}(z)}{\partial z^2} + n^*_{\varepsilon,1}(z)\left(r_1(z) - \kappa_1 N^*_{\varepsilon,1}\right) + m_2 n^*_{\varepsilon,2}(z) - m_1 n^*_{\varepsilon,1}(z), \\ 0 = U\varepsilon^2 \frac{\partial^2 n^*_{\varepsilon,2}(z)}{\partial z^2} + n^*_{\varepsilon,2}(z)\left(r_2(z) - \kappa_2 N^*_{\varepsilon,2}\right) + m_1 n^*_{\varepsilon,1}(z) - m_2 n^*_{\varepsilon,2}(z). \end{cases} \tag{A.19}$$

We first let $\varepsilon \to 0$ in the above equation to obtain that $n^*_{\varepsilon,i}(z) \to n_i(z)$ and $N^*_{\varepsilon,i} \to N_i$ with

$$\begin{cases} 0 = n_1(z)\left(r_1(z) - \kappa_1 N_1\right) + m_2 n_2(z) - m_1 n_1(z), \\ 0 = n_2(z)\left(r_2(z) - \kappa_2 N_2\right) + m_1 n_1(z) - m_2 n_2(z), \\ N_i = \int_{-\infty}^{\infty} n_i(z) dz, \end{cases}$$

which is equivalent with

$$\mathcal{A}(z,N_1,N_2)\begin{pmatrix} n_1(z)\\ n_2(z)\end{pmatrix}=0,\qquad N_i=\int_{-\infty}^{\infty}n_i(z)dz,$$

with $\mathcal{A}(z,N_1,N_2)$ given by (15). This means that (N_1,N_2) corresponds to the sizes of the populations 1 and 2 at the demographic equilibrium $(n_1(z),n_2(z))$, in absence of mutations. We will show that this equilibrium corresponds indeed to a global evolutionary stable strategy and hence $N_i=N_i^*$. To this end, we replace (16) in (A.19) and obtain

$$\begin{cases}0=\varepsilon U\frac{\partial^2 u_{\varepsilon,1}(z)}{\partial z^2}+U|\frac{\partial}{\partial z}u_{\varepsilon,1}(z)|^2+r_1(z)-\kappa_1 N^*_{\varepsilon,1}+m_2\exp(\frac{u_{\varepsilon,2}(z)-u_{\varepsilon,1}(z)}{\varepsilon})-m_1,\\ \\ 0=\varepsilon U\frac{\partial^2 u_{\varepsilon,2}(z)}{\partial z^2}+U|\frac{\partial}{\partial z}u_{\varepsilon,2}(z)|^2+r_2(z)-\kappa_2 N^*_{\varepsilon,2}+m_1\exp(\frac{u_{\varepsilon,1}(z)-u_{\varepsilon,2}(z)}{\varepsilon})-m_2.\end{cases}\tag{A.20}$$

Similarly to above, this system is derived using the following equalities

$$\frac{\partial}{\partial z}n^*_{\varepsilon,i}(z)=\big(\frac{\partial}{\partial z}u_{\varepsilon,i}(z)\big)\frac{n^*_{\varepsilon,i}(z)}{\varepsilon},\qquad \frac{\partial^2}{\partial z^2}n^*_{\varepsilon,i}(z)=\left(\varepsilon\frac{\partial^2}{\partial z^2}u_{\varepsilon,i}(z)+|\frac{\partial}{\partial z}u_{\varepsilon,i}(z)|^2\right)\frac{n^*_{\varepsilon,i}(z)}{\varepsilon^2}.$$

We can determine $u_i(z)$, $v_i(z)$ from the above equation and (17).
Note that the exponential terms in (A.20) suggest that, when $m_i>0$ for $i=1,2$, as $\varepsilon\to 0$ $u_{\varepsilon,1}(z)$ and $u_{\varepsilon,2}(z)$ converge to the same limit $u(z)$. Otherwise, one of these exponential terms tends to infinity while the other terms are bounded. Keeping the zero order terms (the ones in front of which there is no ε, corresponding to the dominant terms) we obtain

$$\begin{cases}0=U|\frac{\partial}{\partial z}u(z)|^2+r_1(z)-\kappa_1 N_1+m_2\exp(v_2(z)-v_1(z))-m_1,\\ 0=U|\frac{\partial}{\partial z}u(z)|^2+r_2(z)-\kappa_2 N_2+m_1\exp(v_1(z)-v_2(z))-m_2.\end{cases}\tag{A.21}$$

We then multiply the first line by $\exp(v_1(z))$ and the second line by $\exp(v_2(z))$ and write the system in the matrix form to obtain, using (14),

$$\begin{pmatrix} w_1(z;N_1)-m_1 & m_2\\ m_1 & w_2(z;N_2)-m_2\end{pmatrix}\begin{pmatrix}\exp(v_1(z))\\ \exp(v_2(z))\end{pmatrix}=-U|\frac{\partial}{\partial z}u(z)|^2\begin{pmatrix}\exp(v_1(z))\\ \exp(v_2(z))\end{pmatrix}.$$

Note that the matrix in the l.h.s. is nothing but $\mathcal{A}(z,N_1,N_2)$ given by (15). The equality above means that $-U|\frac{\partial}{\partial z}u(z)|^2$ is indeed the principal eigenvalue of $\mathcal{A}(z;N_1,N_2)$, that is (see Section 3.2.1)

$$-U|\frac{\partial}{\partial z}u(z)|^2=W(z;N_1,N_2).$$

Similarly to Subsection A.1.1, to have a finite but positive size of population, we should have

$$\max_{z\in\mathbb{R}}u(z)=0.$$

Otherwise, in view of (16), the total population size whether becomes infinite as $\varepsilon\to 0$ (if $\max_{z\in\mathbb{R}}u(z)>0$) or it goes to 0 (if $\max_{z\in\mathbb{R}}u(z)<0$). Similarly we obtain

$$\operatorname{supp} n_i\subset\{z\,|\,u(z)=0\},$$

where $\operatorname{supp} n_i$ is the set of traits z such that the density $n_i(z)$ is positive. The above property holds since $u(z_0) < 0$ implies that $\lim_{\varepsilon\to 0} n^*_{\varepsilon,i}(z_0) = 0$.
Let $\bar{z}$ be such that $u(\bar{z}) = 0$ which means that it is a maximum point of $u(z)$. Then, $\frac{\partial}{\partial z}u(\bar{z}) = 0$ and hence

$$W(\bar{z}; N_1, N_2) = 0.$$

Moreover in all the points $z \in \mathbb{R}$, we have

$$W(z; N_1, N_2) = -U|\frac{\partial}{\partial z}u(z)|^2 \leq 0.$$

This implies that

$$\begin{aligned} &\text{if } z \in \operatorname{supp} n_1 = \operatorname{supp} n_2 \text{ then } W(z; N_1, N_2) = 0,\\ &\text{if } z \notin \operatorname{supp} n_1 = \operatorname{supp} n_2 \text{ then } W(z; N_1, N_2) \leq 0. \end{aligned}$$

In other words $(n_1(z), n_2(z))$ corresponds to the demographic equilibrium corresponding to the global ESS and hence $n_i(z) = n^*_i(z)$ and $N_i = N^*_i$, with $n^*_i(z)$ and N^*_i given in Subsection A.2.1.1.
We gather the informations that we obtained on $u(z)$:

$$\begin{cases} -U|\frac{\partial}{\partial z}u(z)|^2 = W(z; N^*_1, N^*_2),\\ \max_{z\in\mathbb{R}} u(z) = 0, \end{cases} \tag{A.22}$$

with the maximum points of $u(z)$ attained at the ESS points.
This property allows us to provide explicit formula for $u(z)$.
In the case of monomorphic ESS, $u(z)$ is given by

$$u(z) = -\frac{1}{\sqrt{U}}\Big|\int_{z^{M*}}^{z} \sqrt{-W(x; N_1^{M*}, N_2^{M*})}dx\Big|. \tag{A.23}$$

The reader can verify that $u(z)$, given by the formula above, is smooth and solves (A.22) with its maximum point at z^{M*}.
In the case of dimorphic ESS, $u(z)$ is given by

$$u(z) = \max\Big(-\frac{1}{\sqrt{U}}\Big|\int_{z_{\mathrm{I}}^{D*}}^{z} \sqrt{-W(x; N_1^{M*}, N_2^{M*})}dx\Big|, -\frac{1}{\sqrt{U}}\Big|\int_{z_{\mathrm{II}}^{D*}}^{z} \sqrt{-W(x; N_1^{M*}, N_2^{M*})}dx\Big|\Big). \tag{A.24}$$

The reader can also verify that the above function is smooth at all points except at the point where the two functions in the maximum operator intersect. Moreover, $u(z)$ solves (A.22) at the smooth points and it attains its maximum at the ESS points z_{I}^{D*} and z_{II}^{D*}. See Mirrahimi 2017 for the details on why this is indeed the solution obtained at the limit $\varepsilon \to 0$.

Computation of the next order terms $v_i(z)$:
The derivation of the next order terms $v_i(z)$ follows also similar arguments as in Section A.1.1. However, since here we have a system the computations are less straight forward. We present the main ingredients to compute these terms.
From (A.21) and (A.22) we can compute $v_2(z) - v_1(z)$ thanks to the following formula

$$v_2(z) - v_1(z) = \log\Big(\frac{1}{m_2}\big(W(z, N_1^{M*}, N_2^{M*}) - w(z, N_1^{M*}) + m_1\big)\Big).$$

We next keep the first order terms in (A.20), i.e. the terms with an ε in front of them. To do so, we need to go further than (17) in the approximation of $u_{\varepsilon,i}(z)$ and also keep the term of order ε^2, $l_i(z)$:

$$u_{\varepsilon,i}(z) = u(z) + \varepsilon v_i(z) + \varepsilon^2 l_i(z) + O(\varepsilon^3).$$

Then, keeping the first order terms in (A.20) we obtain

$$\begin{cases} 0 = U\frac{\partial^2}{\partial z^2}u(z) + 2U\frac{\partial}{\partial z}u(z)\frac{\partial}{\partial z}v_1(z) - \kappa_1 K_1 + m_2\exp(v_2(z) - v_1(z))(l_2(z) - l_1(z)), \\ 0 = U\frac{\partial^2}{\partial z^2}u(z) + 2U\frac{\partial}{\partial z}u(z)\frac{\partial}{\partial z}v_2(z) - \kappa_2 K_2 + m_2\exp(v_1(z) - v_2(z))(l_1(z) - l_2(z)). \end{cases} \tag{A.25}$$

Using the above equalities and by evaluating them at the ESS points we can compute $v_i(z)$ and K_i for $i = 1, 2$. See Mirrahimi 2017–Section 3.3 for the details of such computations.

A.2.1.3 Derivation of our *second approximation* in presence of migration Explicit formula for the moments of order k, with $k \geq 1$, of the phenotypic distribution, called our *second approximation*, can be derived following similar arguments as in Section A.1.2. However, in presence of migration we should consider two cases of monomorphic and dimorphic population. The case of monomorphic ESS can be treated exactly as in Section A.1.2. The dimorphic case is slightly different and we provide the additional elements to compute the moments of the phenotypic distribution in this case.

Let's suppose that the model has a dimorphic ESS $\{z_{\mathrm{I}}^{D*}, z_{\mathrm{II}}^{D*}\}$ with $N_i^{D*} = \nu_{\mathrm{I,i}} + \nu_{\mathrm{II,i}}$. We first compute the local moments of the phenotypic density, that is, for $k = \mathrm{I}, \mathrm{II}$,

$$\begin{cases} \nu_{\varepsilon,k,i}^{D*} = \int_{\mathcal{O}_k} n_{\varepsilon,i}^{D*}(z)dz, \\ \mu_{\varepsilon,k,i}^{D*} = \frac{1}{\nu_{\varepsilon,k,i}}\int_{\mathcal{O}_k} z n_{\varepsilon,i}^{D*}(z)dz, \\ \sigma_{\varepsilon,k,i}^{D*\,2} = \frac{1}{\nu_{\varepsilon,k,i}}\int_{\mathcal{O}_k}(z - \mu_{\varepsilon,k,i}^{D*})^2 n_{\varepsilon,i}^{D*}(z)dz, \\ \psi_{\varepsilon,k,i}^{D*} = \frac{1}{\nu_{\varepsilon,k,i}^{D*}}\int_{\mathcal{O}_k}(z - \mu_{\varepsilon,k,i}^{D*})^3 n_{\varepsilon,i}^{D*}(z)dz \end{cases}$$

with $\mathcal{O}_{\mathrm{I}} = (-\infty, 0)$ and $\mathcal{O}_{\mathrm{II}} = (0, \infty)$. We can next compute the global moments of the population's distribution from the above local moments.
Since in this case we also need to compute the local population sizes $\nu_{\varepsilon,k,i}^{D*}$, we need to go an order further in the Taylor expansions and also use the value of the second order term l_i at the ESS points z_k^{D*}:

$$u(z) = -\frac{A_k}{2}(z - z_k^{D*})^2 + B_k(z - z_k^{D*})^3 + C_k(z - z_k^{D*})^4 + O(z - z_k^{D*})^5,$$

$$v_i(z) = \log(\sqrt{A_k}\nu_{k,i}) + D_{k,i}(z - z_k^{D*}) + E_{k,i}(z - z_k^{D*})^2 + O(z - z_k^{D*})^3, \qquad l_i(z_k^{D*}) = F_{k,i}.$$

Note that we can compute the Taylor expansions of u and v thanks to the expression of u, given by (A.24), and the expression of v_i, obtained following Section A.2.1.2. Moreover, we can derive the value of $F_{k,i}$ thanks to (A.25).
The above approximation allows us, similarly to Subsection A.1.2, to estimate the local moments of

the population's distribution:

$$\begin{cases} \nu^{D*}_{\varepsilon,k,i} = \nu_{k,i}(1+\varepsilon K_{k,i}) + O(\varepsilon^2), \\ \mu^{D*}_{\varepsilon,k,i} = z^{D*}_k + \varepsilon(\frac{3B_k}{A_k^2} + \frac{D_{k,i}}{A_k}) + O(\varepsilon^2), \\ \sigma^{D*\,2}_{\varepsilon,k,i} = \frac{\varepsilon}{A_k} + O(\varepsilon^2), \\ \psi^{D*}_{\varepsilon,k,i} = \frac{6B_k}{A_k^3}\varepsilon^2 + O(\varepsilon^3), \end{cases} \tag{A.26}$$

with

$$K_{k,i} = F_{k,i} + \frac{E_{k,i} + 0.5D_{k,i}^2}{A_k} + \frac{3(C_k + B_k D_{k,i})}{A_k^2} + \frac{7.5B_k^2}{A_k^3}.$$

Derivation of the analytic formula (A.26)**:**
The above analytic formula for the moments of order $1 \leq k \leq 3$ can be derived following similar arguments as in Section A. To derive the explicit formula for $\nu^{D*}_{\varepsilon,k,i}$ we also use similar type of arguments. We can indeed use the Taylor expansions above to compute

$$\begin{aligned} \nu^{D*}_{\varepsilon,k,i} &= \int_{\mathcal{O}_k} n_{\varepsilon,i}(z)dz \\ &= \frac{\sqrt{A_k}\nu_{k,i}}{\sqrt{2\pi}} \int_{\mathbb{R}} e^{-\frac{A_k}{2}y^2}\big(1 + \sqrt{\varepsilon}(B_k y^3 + D_{k,i}y) + \varepsilon(0.5(B_k y^3 + D_{k,i}y)^2 + C_k y^4 + E_{k,i}y^2 + F_{k,i}) + O(\varepsilon^2)\big)dy \\ &= \nu_{k,i}(1 + \varepsilon(F_{k,i} + \tfrac{E_{k,i}+0.5D_{k,i}^2}{A_k} + \tfrac{3(C_k+B_kD_{k,i})}{A_k^2} + \tfrac{7.5B_k^2}{A_k^3})) + O(\varepsilon^2), \end{aligned}$$

Note that to compute the integral terms above we have performed a change of variable $z - z^{M*} = \sqrt{\varepsilon}y$, therefore each term $z - z^{M*}$ can be considered as of order $\sqrt{\varepsilon}$ in the integrations.

A.2.2 The extreme source and sink case (where $m_1 > 0$ and $m_2 = 0$)

In this section, we provide the derivation of our approximations in the extreme source and sink scenario. In Subsection A.2.2.1 we provide our derivation in the Adaptive Dynamics framework and in Subsection A.2.2.2 we present the analysis for our *first approximation*. We do not provide the derivation of our *second approximation* in the extreme source and sink scenario since it is similar to the general case.

A.2.2.1 Adaptive dynamics in the extreme source and sink scenario We first recall the evolutionary outcome in the first habitat which depends only on selection acting in habitat 1: the ESS is $-\theta$ and

$$N_1^* = \frac{r_{\max,1} - m_1}{\kappa_1}.$$

In the second habitat, a part of the population 1, with trait $-\theta$ and with size $\frac{m_1(r_{\max,1}-m_1)}{\kappa_1}$, is present thanks to migration. The growth rate of any other trait z in this habitat is given by $w_2(z; N_2^*) = r_{\max,2} - s_2(z-\theta)^2 - \kappa_2 N_2^*$. Therefore the only trait, in addition to the trait $z = -\theta$, that can be present at the ESS is the maximum point of $w_2(z; N_2^*)$, that is $z = \theta$. This means that the ESS at the second habitat, is whether monomorphic and given by $\{-\theta\}$ or dimorphic and given by $\{-\theta, \theta\}$. The dimorphism in the second habitat occurs if the trait θ is strong enough to compete with the

maladapted trait $-\theta$ coming from the first habitat. This occurs under the following condition:

$$\frac{m_1(r_{\max,1}-m_1)}{\kappa_1} < \frac{4s_2\theta^2 r_{\max,2}}{\kappa_2}. \tag{A.27}$$

Under this condition, there exists indeed a positive demographic equilibrium for the set of traits $\{-\theta,\theta\}$:

$$n_2^{D*} = \alpha\delta(z+\theta)+\beta\delta(z-\theta), \quad N_2^{D*} = \alpha+\beta = \frac{r_2}{\kappa_2},$$

such that

$$m_1N_1^* + w_2(-\theta;N_2^{D*})\alpha = 0, \qquad w_2(\theta;N_2^{D*})\beta = 0.$$

We can indeed compute the densities α, β and N_2^{D*}:

$$N_2^{D*} = \frac{r_2}{\kappa_2}, \qquad \alpha = \frac{m_1(r_{\max,1}-m_1)}{4s_2\theta^2\kappa_1}, \quad \beta = \frac{r_{\max,2}}{\kappa_2} - \frac{m_1(r_{\max,1}-m_1)}{4s_2\theta^2\kappa_1}.$$

When the condition (A.27) is not satisfied, then there is no such demographic equilibrium. The ESS is then monomorphic with trait $-\theta$ and the demographic equilibrium is given by

$$n_2^{M*} = N_2^*\,\delta(z+\theta), \qquad m_1N_1^* + w_2(\theta;N_2^{M*})N_2^{M*} = 0,$$

leading to

$$N_2^{M*} = \frac{1}{2\kappa_2}\Big(r_2 - 4s_2\theta^2 + \sqrt{(r_{\max,2}-4s_2\theta^2)^2 + 4\frac{\kappa_2}{\kappa_1}m_1(r_{\max,1}-m_1)}\Big).$$

To understand the relation with Section A.2.1.1, note that the above computations are equivalent with finding an ESS for the effective growth rate $W(z;N_1^*,N_2^*)$, corresponding to the principal eigenvalue of $\mathcal{A}(z;N_1^*,N_2^*)$ which is given by

$$W(z;N_1^*,N_2^*) = \max\big(w_1(z;N_1^*)-m_1, w_2(z;N_2^*)\big),$$

as a consequence of $m_2 = 0$.

A.2.2.2 Derivation of the *first approximation* in the extreme source and sink scenario

The population's phenotypic density $n_{\varepsilon,1}^*$ can be computed explicitly as in Subsection 3.1.2, the example of quadratic growth rate: $n_{\varepsilon,1}^* = N_{\varepsilon,1}^* f_\varepsilon$, where $N_{\varepsilon,1}^* = \frac{r_{\max,1}-m_1-\varepsilon\sqrt{Us_1}}{\kappa_1}$ and f_ε is the probability density of a normal distribution $\mathcal{N}(-\theta, \frac{\varepsilon\sqrt{U}}{\sqrt{s_1}})$. This allows us to compute $u_{\varepsilon,1}$, given by (16):

$$u_{\varepsilon,1} = -\frac{\sqrt{s_1}(z+\theta)^2}{2\sqrt{U}} + \varepsilon\log\left(s_1^{\frac{1}{4}}\Big(N_1^* - \varepsilon\frac{\sqrt{Us_1}}{\kappa_1}\Big)\right),$$

and hence

$$u_{\varepsilon,1} = u_1 + \varepsilon v_1 + \varepsilon^2 l_1 + o(\varepsilon^2), \qquad N_{\varepsilon,1} = N_1^* + \varepsilon K_1 + o(\varepsilon),$$

with

$$u_1 = -\frac{\sqrt{s_1}(z+\theta)^2}{2\sqrt{U}}, \qquad v_1 \equiv \log\big(s_1^{\frac{1}{4}}N_1^*\big), \qquad l_1 \equiv -\frac{\sqrt{Us_1}}{\kappa_1 N_1^*}, \qquad K_1 = -\frac{\sqrt{Us_1}}{\kappa_1}. \tag{A.28}$$

To estimate the phenotypic density in the second habitat we study the equation on $u_{\varepsilon,2}$ given by (16) and (A.20):

$$0 = \varepsilon U \frac{\partial^2 u_{\varepsilon,2}(z)}{\partial z^2} + U|\frac{\partial}{\partial z} u_{\varepsilon,2}(z)|^2 + r_2(z) - \kappa_2 N^*_{\varepsilon,2} + m_1 \exp(\frac{u_{\varepsilon,1}(z) - u_{\varepsilon,2}(z)}{\varepsilon}). \tag{A.29}$$

Note that here we have used the fact that $m_2 = 0$. As above we expect to have an asymptotic expansion for $u_{\varepsilon,2}(z)$ and $N^*_{\varepsilon,2}$:

$$u_{\varepsilon,2}(z) = u_2(z) + \varepsilon v_2(z) + \varepsilon^2 l_2(z) + o(\varepsilon^2), \qquad N^*_{\varepsilon,2} = N^*_2 + \varepsilon K_2.$$

Derivation of $u_2(z)$.
We replace the above expansion in (A.29). From the exponential term in (A.29) we deduce that

$$u_2(z) \geq u_1(z).$$

Otherwise this exponential term will tend to infinity. However, unlike Section A.2.1.2, here we don't have necessarily that $u_1(z) \geq u_2(z)$, which means that we don't have necessarily $u_1(z) = u_2(z)$. This is because $m_2 = 0$ and there is no such exponential term in the equation on $u_{\varepsilon,1}(z)$. This is why the source and sink case is a degenerate case comparing to what we studied in Section A.2.1.2.
In order to identify $u_2(z)$ we first notice that keeping the ε^0 order terms in (A.29) and using the positivity of the exponential term in (A.29), we obtain that, for all $z \in \mathbb{R}$,

$$-U|u_2'(z)|^2 \geq r_2(z) - \kappa_2 N^*_2. \tag{A.30}$$

Next, we consider two cases:
(i) Let z be such that $u_1(z) < u_2(z)$. In this case, $\exp\left(\frac{u_{\varepsilon,1}(z) - u_{\varepsilon,2}(z)}{\varepsilon}\right)$ tends to 0, and keeping the ε^0 order terms in (A.29) we obtain

$$-U|u_2'(z)|^2 = r_2(z) - \kappa_2 N^*_2. \tag{A.31}$$

(ii) Let z be such that $u_1(z) = u_2(z)$. Assuming that the equality holds on an open interval including z, we can write

$$-U|u_2'(z)|^2 = -U|u_1'(z)|^2 = r_1(z) - \kappa_1 N^*_1 - m_1. \tag{A.32}$$

Thanks to (A.30) and (A.32) we deduce in particular that if at some trait z_0,

$$r_1(z_0) - \kappa_1 N^*_1 - m_1 < r_2(z_0) - \kappa_2 N^*_2,$$

then $u_1(z_0) \neq u_2(z_0)$ and hence u_2 solves (A.31) at z_0.
Combining the above properties we can determine the equation on u_2. To this end, we consider three cases:
(1) Let $s_2 < s_1$. In this case, there exists (z_1, z_2) such that $z_1 < -\theta < z_2 < \theta$ and

$$r_1(z) - \kappa_1 N^*_1 - m_1 \geq r_2(z) - \kappa_2 N^*_2, \qquad \text{for } z \in [z_1, z_2],$$

and

$$r_1(z) - \kappa_1 N^*_1 - m_1 < r_2(z) - \kappa_2 N^*_2, \qquad \text{for } z \in (-\infty, z_1) \cup (z_2, \infty).$$

This leads to the following equation on $u_2(z)$:

$$-U|u_2'(z)|^2 = g_1(z) := \max\big(r_2(z) - \kappa_2 N_2^*, r_1(z) - \kappa_1 N_1^* - m_1\big).$$

(2) Let $s_1 < s_2$. In this case, there exists (z_1, z_2) such that $-\theta < z_1 < \theta < z_2$ and

$$r_1(z) - \kappa_1 N_1^* - m_1 \le r_2(z) - \kappa_2 N_2^*, \qquad \text{for } z \in [z_1, z_2],$$

and

$$r_1(z) - \kappa_1 N_1^* - m_1 > r_2(z) - \kappa_2 N_2^*, \qquad \text{for } z \in (-\infty, z_1) \cup (z_2, \infty).$$

This leads to the following equation on $u_2(z)$:

$$-U|u_2'(z)|^2 = g_2(z),$$

with $g_2(z)$ given by

$$g_2(z) = \begin{cases} r_1(z) - \kappa_1 N_1^* - m_1, & \text{if } z \le z_1, \\ r_2(z) - \kappa_2 N_2^*, & \text{if } z > z_1. \end{cases}$$

(3) Let $s_1 = s_2$. In this case, there exists a point z_1 such that $-\theta < z_1 < \theta$ and

$$r_1(z) - \kappa_1 N_1^* - m_1 \ge r_2(z) - \kappa_2 N_2^*, \qquad \text{for } z \in (-\infty, z_1],$$

and

$$r_1(z) - \kappa_1 N_1^* - m_1 < r_2(z) - \kappa_2 N_2^*, \qquad \text{for } z \in (z_1, \infty).$$

This leads to the following equation on $u_2(z)$:

$$-U|u_2'(z)|^2 = g_3(z),$$

with

$$g_3(z) = g_1(z) = \max\big(r_2(z) - \kappa_2 N_2^*, r_1(z) - \kappa_1 N_1^* - m_1\big).$$

From the above formula we can determine $u_2(z)$:
Monomorphic case: Under condition

$$\frac{4 s_2 \theta^2 r_{\max,2}}{\kappa_2} < \frac{m_1(r_{\max,1} - m_1)}{\kappa_1},$$

the functions $g_i(z)$ have a unique maximum point at $-\theta$. This means in particular that the ESS is monomorphic (see condition (21)). This leads to the following formula for $u_2(z)$

$$u_2(z) = -\frac{1}{\sqrt{U}} \Big| \int_{-\theta}^{z} \sqrt{-g_i(x)}\, dx \Big|^2, \tag{A.33}$$

where we use g_i, with $i = 1, 2, 3$, for case (i).
Dimorphic case: Under condition

$$\frac{4 s_2 \theta^2 r_{\max,2}}{\kappa_2} > \frac{m_1(r_{\max,1} - m_1)}{\kappa_1},$$

the functions $g_i(z)$ have two maximum points at $-\theta$ and θ. This means that the ESS is dimorphic and $z_1^{D*} = -z_2^{D*} = -\theta$. Moreover, the function $u_2(z)$ can be computed as below

$$u_2(z) = \max\Big(-\frac{1}{\sqrt{U}} \Big| \int_{-\theta}^{z} \sqrt{-g_i(x)}dx \Big|^2, -\frac{1}{\sqrt{U}} \Big| \int_{\theta}^{z} \sqrt{-g_i(x)}dx \Big|^2 \Big), \tag{A.34}$$

where we use g_i, with $i = 1, 2, 3$, for case (i).

Derivation of $v_2(z)$.
To compute the next order term $v_2(z)$, we also consider two cases:
(i) Let z be such that $u_1(z) < u_2(z)$. As above, in this case, $\exp\big(\frac{u_{\varepsilon,1}(z) - u_{\varepsilon,2}(z)}{\varepsilon}\big)$ tends to 0, and keeping the ε order terms in (A.29) we obtain

$$-U\, u_2''(z) = 2U\, u_2'(z) v_2'(z) - \kappa_2 K_2.$$

Since we have already computed the expression for $u_2(z)$ ((A.33) and (A.34)) we can compute $v_2'(z)$ (and hence $v_2(z)$) from the above formula. In particular, in the dimorphic case, the computations are straight forward. In this case $u_2'(z)$ is given by (A.31) with $r_2(z) - \kappa_2 N_2^* = -s_2(z-\theta)^2$. Therefore,

$$u_2'(z) = -\frac{\sqrt{s_2}}{\sqrt{U}}\,(z-\theta), \qquad u_2''(z) = -\frac{\sqrt{s_2}}{\sqrt{U}}.$$

Combining the above equalities we obtain that $v_2'(z) = 0$, and hence $v_2(z)$ is constant in this zone:

$$v_2(z) = v_2(\theta), \qquad K_2 = -\frac{\sqrt{U s_2}}{\kappa_2}.$$

(ii) Let z be such that $u_1(z) = u_2(z)$. Then, keeping the ε^0 order terms in (A.29) we obtain

$$-U|u_2'(z)|^2 = r_2(z) - \kappa_2 N_2^* + m_1 \exp(v_1(z) - v_2(z)).$$

Since $u_2(z)$ and $v_1(z)$ are already given by (A.33), (A.34) and (A.28), the above formula allows us to compute $v_2(z)$:

$$v_2(z) = v_1(z) - \log\left(\frac{r_1(z) - \kappa_1 N_1^* - m_1 - r_2(z) + \kappa_2 N_2^*}{m_1} \right).$$

The above computations are relevant for z far from the point $\bar{z}_0$ such that

$$r_1(\bar{z}_0) - \kappa_1 N_1^* - m_1 = r_2(\bar{z}_0) - \kappa_2 N_2^*.$$

From the expression of $v_2(z)$ above we notice indeed that there is a singularity at the point $\bar{z}_0$ since the value inside the logarithmic term vanishes at $\bar{z}_0$. This shows that such approximation does not hold close to the point $\bar{z}_0$. In our numerical simulations in Figure 6 we use indeed a linear approximation of the formula above for $v_2(z)$ which provides already convincing results.

A.3 Derivation of a Hamilton-Jacobi equation in the case of model (2)

Our approach can also be used to study the more general model (2). The objective would be to provide an approximation of the equilibrium solution n_i^* when the variance of the mutation distribution is small.

We assume indeed that the variance of the mutation distribution K_ε scales as $\varepsilon^2 V_0$. More precisely, we assume that $K_\varepsilon(y)dy = K(\frac{y}{\varepsilon})\frac{dy}{\varepsilon}$ (for instance a Gaussian distribution with mean 0 and variance $\varepsilon^2\sigma^2$ has such form). Then, the stationary version of (2) may be written as

$$\begin{aligned} 0 \quad &= U\big(\int_{-\infty}^{+\infty} n^*_{\varepsilon,i}(z-\varepsilon y)K(y)dy - n^*_{\varepsilon,i}(z)\big) + n^*_{\varepsilon,i}(z)\left(r_i(z) - \kappa_i \int_{-\infty}^{+\infty} n^*_{\varepsilon,i}(t,y)dy\right) \\ &\quad + m_j n^*_{\varepsilon,j}(z) - m_i n^*_{\varepsilon,i}(z). \end{aligned}$$

Next, analogously to our work in the case of (3), we use the ansatz (16):

$$n^*_{\varepsilon,i} = \frac{1}{2\pi\varepsilon}\exp\big(\frac{u_{\varepsilon,i}}{\varepsilon}\big)$$

and postulate an expansion for $u_{\varepsilon,i}$ in terms of ε:

$$u_{\varepsilon,i} = u_i + \varepsilon v_i + O(\varepsilon^2).$$

The computation of the above terms allows us to provide approximations of the population phenotypic densities $n^*_{\varepsilon,i}(z)$ and their moments. To compute these terms, analogously to what we presented for the diffusion case, thanks to the combination of the above equalities, we derive some equations satisfied by u_i and v_i. The resolution of such equations, which is less straight forward comparing to the diffusion case, allows us to compute these terms. We provide here, the equation satisfied by the zero order term u_i. To this end, we replace (16) in the above equation to obtain

$$\begin{cases} -U\int_{-\infty}^{+\infty}\big(e^{\frac{u_{\varepsilon,1}(z-\varepsilon y)-u_{\varepsilon,1}(z)}{\varepsilon}} - 1\big)K(y)dy = r_{\max,1} - \kappa_1 N^*_{\varepsilon,1} + m_2\exp(\frac{u_{\varepsilon,2}-u_{\varepsilon,1}}{\varepsilon}) - m_1, \\ \\ -U\int_{-\infty}^{+\infty}\big(e^{\frac{u_{\varepsilon,2}(z-\varepsilon y)-u_{\varepsilon,2}(z)}{\varepsilon}} - 1\big)K(y)dy = r_{\max,2} - \kappa_2 N^*_{\varepsilon,2} + m_1\exp(\frac{u_{\varepsilon,1}-u_{\varepsilon,2}}{\varepsilon}) - m_2. \end{cases}$$

Similarly to Subsection A.2.1.2, the exponential terms, coming from the migration terms, suggest that when $m_i > 0$ for $i = 1, 2$, as $\varepsilon \to 0$, $u_{\varepsilon,1}$ and $u_{\varepsilon,2}$ converge to the same limit u. The limit u solves the following Hamilton-Jacobi equation

$$\begin{cases} -U\int_{-\infty}^{+\infty}\big(e^{-y\frac{\partial}{\partial z}u(z)} - 1\big)K(y)dy = W(z; N^*_1, N^*_2), \\ \max_{z\in\mathbb{R}} u(z) = 0, \end{cases} \tag{A.35}$$

where (N^*_1, N^*_2) is the demographic equilibrium corresponding to the ESS and W is the largest eigenvalue of matrix $\mathcal{A}$ (i.e. the effective fitness introduced in Section 3.2.1). See Barles et al. 2009 where the details of such computations are provided in the case of a homogeneous environment.

B Some expressions for the case studies

B.1 Local densities in the dimorphic case for general and symmetric scenarios

In this section, we provide the expressions of the local densities in the dimorphic case in the Adaptive Dynamics framework and for the general non-symmetric scenario with $m_i > 0$. The expressions of the local densities in the symmetric case can be obtained from the same formula, using $m_1 = m_2 =$

$m, \kappa_1 = \kappa_2 = \kappa, s_1 = s_2 = g, r_{\max,1} = r_{\max,2} = r_{\max}$.
To this end, we first recall the values of the global densities at the ESS:

$$N_1^{D*} = \frac{\frac{m_1 m_2}{4\theta^2 s_2} + r_{\max,1} - m_1}{\kappa_1}, \qquad N_2^{D*} = \frac{\frac{m_1 m_2}{4\theta^2 s_1} + r_{\max,2} - m_2}{\kappa_2}.$$

Then the local densities $\nu_{k,i}$, for $k = \mathrm{I}, \mathrm{II}$ and $i = 1, 2$, are given by

$$\begin{pmatrix} \nu_{\mathrm{I},1} \\ \nu_{\mathrm{I},2} \end{pmatrix} = \frac{m_1 N_1^{D*} + (w_2(z^{D*}; N_2^{D*}) - m_2) N_2^{D*}}{m_1 m_2 - \big(w_1(-z^{D*}; N_1^{D*}) - m_1\big)\big(w_2(z^{D*}; N_2^{D*}) - m_2\big)} \begin{pmatrix} m_2 \\ -w_1(-z^{D*}; N_1^{D*}) + m_1 \end{pmatrix},$$
$$\begin{pmatrix} \nu_{\mathrm{II},1} \\ \nu_{\mathrm{II},2} \end{pmatrix} = \frac{m_2 N_2^{D*} + (w_1(-z^{D*}; N_1^{D*}) - m_1) N_1^{D*}}{m_1 m_2 - \big(w_1(-z^{D*}; N_1^{D*}) - m_1\big)\big(w_2(z^{D*}; N_2^{D*}) - m_2\big)} \begin{pmatrix} -w_2(z^{D*}; N_2^{D*}) + m_2 \\ m_1 \end{pmatrix}.$$

B.2 Condition for dimorphism in a general non-symmetric scenario

We provide below the expressions of the constants α_i, β_i and η_i which appear in the condition for dimorphism in Section 3.2.3 in the general non-symmetric scenario (see also Subsection A.2.1.1):

$$\alpha_1 = \frac{2 s_1 \theta}{\kappa_1}\Big(\theta - \sqrt{\theta^2 - \frac{m_1 m_2}{4\theta^2 s_1 s_2}}\Big), \qquad \alpha_2 = \frac{2 s_2 \theta}{\kappa_2}\Big(\theta - \sqrt{\theta^2 - \frac{m_1 m_2}{4\theta^2 s_1 s_2}}\Big),$$

$$\beta_1 = \frac{m_1}{\kappa_1}, \qquad \beta_2 = \frac{m_2}{\kappa_2},$$

$$\eta_1 = \frac{m_2^2}{\kappa_2} + \frac{2 s_1 \theta}{\kappa_1}\Big(\theta - \sqrt{\theta^2 - \frac{m_1 m_2}{4\theta^2 s_1 s_2}}\Big)\Big(\frac{m_1 m_2}{4\theta^2 s_2} - m_1\Big) - \frac{m_1 m_2^2}{4\theta^2 s_1 \kappa_2},$$

$$\eta_2 = \frac{m_1^2}{\kappa_1} + \frac{2 s_2 \theta}{\kappa_2}\Big(\theta - \sqrt{\theta^2 - \frac{m_1 m_2}{4\theta^2 s_1 s_2}}\Big)\Big(\frac{m_1 m_2}{4\theta^2 s_1} - m_2\Big) - \frac{m_1^2 m_2}{4\theta^2 s_2 \kappa_1}.$$

B.3 Analytic formula for the moments of the dimorphic phenotypic distribution in the symmetric case

We provide below our analytic approximations of the local moments of the phenotypic distribution, in the dimorphic case, for both the symmetric scenario and the source and sink scenario. Such local moments are defined in Subsection A.2.1.3). One can compute the global moments of the population's distribution from such local moments.

For the symmetric scenario, we define $\gamma = \sqrt{1 - \frac{m^2}{4s^2\theta^4}}$. Our approximation is then given by

$$\begin{cases} N^{D*}_{\varepsilon,1} = N^{D*}_{\varepsilon,2} = \frac{1}{\kappa}\left(\frac{m^2}{4s\theta^2} + r_{\max} - m\right) - \varepsilon\,\frac{\sqrt{U\,s}\gamma}{\kappa} + O(\varepsilon^2), \\ \mu^{D*}_{\varepsilon,\mathrm{I},1} = z^{D*}_{\mathrm{I}} + \varepsilon\sqrt{U}\big(\frac{m^2}{4s^2\sqrt{s}\theta^5\gamma^2} - \frac{4s^2\theta^4(1-\gamma)^2}{\theta\sqrt{s}\gamma(4s^2\theta^4(1-\gamma)^2+m^2)}\big) + O(\varepsilon^2), \\ \mu^{D*}_{\varepsilon,\mathrm{I},2} = z^{D*}_{\mathrm{I}} + \varepsilon\sqrt{U}\big(\frac{m^2}{4s^2\sqrt{s}\theta^5\gamma^2} + \frac{m^2}{\theta\sqrt{s}\gamma(4s^2\theta^4(1-\gamma)^2+m^2)}\big) + O(\varepsilon^2), \\ \mu^{D*}_{\varepsilon,\mathrm{II},1} = z^{D*}_{\mathrm{II}} - \varepsilon\sqrt{U}\big(\frac{m^2}{4s^2\sqrt{s}\theta^5\gamma^2} + \frac{m^2}{\theta\sqrt{s}\gamma(4s^2\theta^4(1-\gamma)^2+m^2)}\big) + O(\varepsilon^2), \\ \mu^{D*}_{\varepsilon,\mathrm{II},2} = z^{D*}_{\mathrm{II}} - \varepsilon\sqrt{U}\big(\frac{m^2}{4s^2\sqrt{s}\theta^5\gamma^2} - \frac{4s^2\theta^4(1-\gamma)^2}{\theta\sqrt{s}\gamma(4s^2\theta^4(1-\gamma)^2+m^2)}\big) + O(\varepsilon^2), \\ \sigma^{D*\,2}_{\varepsilon,\mathrm{I},1} = \sigma^{D*\,2}_{\varepsilon,\mathrm{I},2} = \sigma^{D*\,2}_{\varepsilon,\mathrm{II},1} = \sigma^{D*\,2}_{\varepsilon,\mathrm{II},2} = \frac{\varepsilon\sqrt{U}}{\sqrt{s}\gamma} + O(\varepsilon^2), \\ \psi^{D*}_{\varepsilon,\mathrm{I},i} = \frac{m^2U\varepsilon^2}{4s^3\theta^5\gamma^3} + O(\varepsilon^3), \\ \psi^{D*}_{\varepsilon,\mathrm{II},i} = -\frac{m^2U\varepsilon^2}{4s^3\theta^5\gamma^3} + O(\varepsilon^3), \end{cases}$$

where the subscripts I and II indicate that the local moments are in the sets $\mathcal{O}_{\mathrm{I}} = (-\infty, 0)$ and $\mathcal{O}_{\mathrm{II}} = (0, \infty)$ which include respectively z^D_{I} and z^D_{II}.

B.4 Some expressions for the source and sink scenario

When the condition (21) holds, the evolutionary equilibrium is monomorphic and the evolutionary stable strategy is $z^* = -\theta$ and the total population size is given by

$$N^*_2 = \frac{1}{2\kappa_2}\Big(r_{\max,2} - 4s_2\theta^2 + \sqrt{(r_{\max,2} - 4s_2\theta^2)^2 + 4\frac{\kappa_2}{\kappa_1}m_1(r_{\max,1} - m_1))}\Big).$$

There is indeed a population of size N^*_2 in the second habitat which is of type $z^* = -\theta$: this population is very maladapted.
Our *second approximation* provides analytic formula for the moments of the phenotypic distribution in the sink (see Figure 6 for a comparison between the first and the second approximations):

$$\begin{cases} N^{M*}_{\varepsilon,2} = N^*_2 - \varepsilon\frac{\sqrt{U}\,m_1N^*_1N^*_2}{m_1N^*_1+\kappa_2N^{*2}_2}\big(-\frac{\sqrt{s_1}}{\kappa_1N^*_1} - \frac{N^*_2\sqrt{s_1}}{m_1N^*_2} + \frac{(s_2-s_1)(r_{\max,2}-\kappa_2N^*_2)+4s_2(s_1+3s_2)\theta^2}{(\kappa_2N^*_2-r_{\max,2}+4s_2\theta^2)^2\sqrt{s_1}}\big) + O(\varepsilon^2), \\ \mu^{M*}_{\varepsilon,2} = -\theta + \varepsilon\frac{4\sqrt{U}\,s_2\theta}{\sqrt{s_1}\big(\kappa_2N^*_2-r_{\max,2}+4s_2\theta^2\big)} + O(\varepsilon^2), \\ \sigma^{M*\,2}_{\varepsilon,2} = \frac{\varepsilon\sqrt{U}}{\sqrt{s_1}} + O(\varepsilon^2), \\ \psi^{M*}_{\varepsilon,2} = O(\varepsilon^3). \end{cases}$$

When the condition (21) is not satisfied, the evolutionary equilibrium is dimorphic in the second habitat:

$$n^*_2 = \nu_{\mathrm{I},2}\delta(z+\theta) + \nu_{\mathrm{II},2}\delta(z-\theta),$$

with

$$\nu_{\mathrm{I},2} = \frac{m_1(r_{\max,1}-m_1)}{4s_2\theta^2\kappa_1}, \qquad \nu_{\mathrm{II},2} = \frac{r_{\max,2}}{\kappa_2} - \frac{m_1(r_{\max,1}-m_1)}{4s_2\theta^2\kappa_1}), \qquad \nu_{\mathrm{I},2} + \nu_{\mathrm{II},2} = N^*_2 = \frac{r_{\max,2}}{\kappa_2}.$$

Then, the moments of the population's distribution in this habitat can be approximated as below:

$$\begin{cases} N_{\varepsilon,2}^{D*} = N_2^* - \varepsilon \frac{\sqrt{U s_2}}{\kappa_2} + O(\varepsilon^2), \\ \mu_{\varepsilon,\mathrm{I},2}^{D*} = -\theta + \varepsilon \frac{\sqrt{U}}{\theta\sqrt{s_1}} + O(\varepsilon^2), \\ \mu_{\varepsilon,\mathrm{II},2}^{D*} = \theta + O(\varepsilon^2), \\ \sigma_{\varepsilon,\mathrm{I},2}^{D*\,2} = \frac{\varepsilon\sqrt{U}}{\sqrt{s_1}} + O(\varepsilon^2), \\ \sigma_{\varepsilon,\mathrm{II},2}^{D*\,2} = \frac{\varepsilon\sqrt{U}}{\sqrt{s_2}} + O(\varepsilon^2), \\ \psi_{\varepsilon,\mathrm{I},2}^{D*} = \psi_{\varepsilon,\mathrm{II},2}^{D*} = O(\varepsilon^3). \end{cases}$$

References

Barles, G., Mirrahimi, S., and Perthame, B. (2009). Concentration in Lotka-Volterra parabolic or integral equations: a general convergence result. *Methods Appl. Anal.*, 16(3):321–340.

Mirrahimi, S. (2017). A Hamilton-Jacobi approach to characterize the evolutionary equilibria in heterogeneous environments. *Math. Models Methods Appl. Sci.*, 27(13):2425–2460.